Polymer Testing

Influence of topographical features on the surface appearance measurement of injection moulded components.

--Manuscript Draft--

Manuscript Number:	POTE_2020_1767R1
Article Type:	Research Paper
Section/Category:	Functional polymer,mechanical properties,thermal analysis,microscopy,self-healing polymer,shape-memo
Keywords:	Injection moulding; Reflectivity contrast; Micro roughness; Surface appearance
Corresponding Author:	Miguel Sanchez-Soto Centre Catala del Plastic. Universitat Politécnica de Catalunya Terrassa, Barcelona Spain
First Author:	Pablo Gamonal Repiso
Order of Authors:	Pablo Gamonal Repiso
	Miguel Sanchez-Soto
	Tobias Abt
	Soledad Santos-Pinto
	LLuisa Maspoch
Abstract:	Adding textures to surfaces is known to improve the external appearance of injection moulded components. However, when high surface quality is required, normally a paint coating is applied on top of the moulded textured surface. In this work, an alternative to painting for obtaining high quality surfaces is proposed, following an environmental-friendly process and having low production cost. Three different surface textures obtained by injection moulding have been characterized and compared with a painted one. Alternative topographical parameters such as the absolute functional height (AFH), the functional height distribution (FHD), texture slope (TS) or texture aperture angle (TAA) besides to the traditional roughness parameters such as the arithmetical mean height (Sa) and the root mean square height (Sq) have been utilized to characterize the random surface textures. The relationships between these parameters and the surface quality appearance represented by gloss and reflectivity contrast have been established using a new total appearance measurement (TAM) apparatus. It was found that by applying secondary operation on the textured mould cavity, such as adding micro roughness features or coatings, equal apparent quality to the ones obtained by painting can be reached.
Suggested Reviewers:	Mikael Rigdahl mikael.rigdahl@chalmers.se Mikael Rigdahl's research interests are primarily within rheology of solids and fluids, composite materials (incl. nanocomposites), renewable materials and the relations between material properties and how we perceive them, e. visually.
	Zoltan Major zoltan.major@jku.at Professor Zoltan Major is an expert in Polymer engineering. Characterization techniques. Friction and Surface properties.
	MOHD FADZLI BIN ABDOLLAH mohdfadzli@utem.edu.my Mr. Mohd is an expert in Friction and Wear of Materials, Surface Engineering and Lubrication
Opposed Reviewers:	
Response to Reviewers:	Editor and Reviewer comments: Reviewer #2:

Powered by Editorial Manager® and ProduXion Manager® from Aries Systems Corporation

	•This is a nice analysis of the surface appearance of injecton molded surfaces I am missing a good graphical overview/summary of the influence parameters, you are providing some explanations but due to the primarily graphical/visual nature of your paper a nice graphical summary would be better/impressive Thanks for the recommendation. A new figure has been included in the manuscript for the better understanding of the influence of the surface parameters on the reflectivity properties. “Fig. 4 depicts the influence of each functional parameter on the surface reflectivity properties. Surfaces with deep valleys (Svk) yield high reflectivity contrast with peaks (light area) due to the reflected light coming from valleys is blocked, creating a dark area. On the contrary, surfaces where the core roughness (Sk) prevails over all functional parameters, lower reflectivity contrast is expected between valleys and peaks. This is because the blocked light coming from valleys is reduced, leading to higher light area as compared to the dark one.” •The citation "Fechner was the first in introducing the word psychophysics and published several studies on perception [2].", you should use the original publication or change the text, as it was descibed by Pelli and Bex .... Thank you for your recommendation. The text has been modified as follows: “In 1860 Fechner introduced the word psychophysics in his entitled book, Elemente der Psychophysik [Fechner, GT. Elemente der Psychophysik. 1860. Leipzig: Breitkopf und Hertel. In: Adler, HE., editor. Elements of Psychophysics. Holt, Rinehart, and Winston; New York: 1860/1966. 1966]. Consequently, several studies were published on perception [2] which meant the beginning of the modern era in the perception-detection field.” •You should provide some information about the filters used (L, S etc) Thank you for your comment. The filters have been described as follows: “The S-filter was utilized for removing the short spatial wavelength or small features of the topography. The L-filter was employed to remove the large spatial wavelength (large features) and the F-Operator was used to remove the base form or the geometrical surface component. The combination of these three filters yielded SF or SL surfaces as defined by the standard ISO 25178-2 [37]. The SF-surface was derived by removing the lateral components (surface features) smaller than the selected S-filter and larger than the F-Operator value, whereas the SL-surface was the result of applying the L-filter on the previously defined SF-surface. Filtering by feature size yielded a better topography perceptibility for a given scale, leading to an adequate separation of the three surface components [38].” •I would change the structure of your paper a bit and describe and define in the experimental part all of your parameters (FHD, TS, TAA) together with the or after the conventional surface roughness parameters used. Than I would describe and discuss the results in the Results chapter. I do not find a proper definition of FHD (mentioned in the Abstract and next in 3.3.1 results ?) you are stating the importance of these parameters in the abstract and in the introduction, a good summary of all definitions would help to understand their importance. Thank you for your comment, the paper structure was slightly modified and the definition of the novel parameters introduced were included in the method part as follows: “The relationship between the surface topography and its reflectance properties was established through the introduction of four novel parameters. The absolute functional height (AFH), the functional height distribution (FHD), the texture slope (TS) and the texture aperture angle (TAA). The AFH is defined as the sum of the three above described functional parameters (Spk + Sk + Svk). This parameter allows determining the averaged texture depth within the sampling area. The FHD allows determining the relative amount of each functional parameter, providing information about which functional parameter prevail on the overall topography, having textures where peaks predominate over valleys or vice versa. Fig. 4 depicts the influence of each functional parameter on the surface reflectivity properties. Surfaces with deep valleys (Svk) yield high reflectivity contrast with peaks (light area) due to the reflected light coming from

	valleys is blocked, creating a dark area. On the contrary, surfaces where the core roughness (Sk) prevails over all functional parameters, lower reflectivity contrast is expected between valleys and peaks. This is because the blocked light coming from valleys is reduced, leading to higher light area as compared to the dark one. The TS is described as the angle formed between the grain surface and its horizontal (underlying surface) and the TAA is the angle between two consecutive grain surfaces. Both TS and TAA were measured as shown in Fig. 5. These two parameters helped to understand the importance of valleys on the light reflectivity performance of a given texture." • On the other hand your are describing in detail Sa, Sq but there are not pointed out in the abstract. The parameters Sa and Sq have been pointed out in the abstract as follows: "Alternative topographical parameters such as the absolute functional height (AFH), the functional height distribution (FHD), texture slope (TS) or texture aperture angle (TAA) besides to the traditional roughness parameters such as the arithmetical mean height (Sa) and the root mean square height (Sq) have been utilized to characterize the random surface textures." •I am speculation about the randomness or regularity of your multiscale structures, could you create a combinaed parameter/explanation for providing a scale (from 0 to 1) to the randomness at various scales Thank you for your comment and contribution. The degree of randomness/isotropy of the surface has been quantified using spatial parameters such as the autocorrelation function (ACF), autocorrelation length (Sal) and the texture aspect ratio (Str). The manuscript has been modified in the materials and methods and results chapters in order to define and discuss these parameters and the obtained results.

Powered by Editorial Manager® and ProduXion Manager® from Aries Systems Corporation

Dear Editor,

Thank you for allowing us to resubmit the article to *Polymer Testing*. We have reworked the manuscript in accordance to reviewer's comments changing text, adding tables and figures as requested.

The point-by-point answers to the reviewer comments are included below. Corrections in the paper have been highlighted in yellow.

We expect that the new version will be within the quality standard of the journal.

Sincerely

Miguel Sánchez-Soto

Editor and Reviewer comments:

Reviewer #2:

- This is a nice analysis of the surface appearance of injecton molded surfaces I am missing a good graphical overview/summary of the influence parameters, you are providing some explanations but due to the primarily graphical/visual nature of your paper a nice graphical summary would be better/impressive

Thanks for the recommendation. A new figure has been included in the manuscript for the better understanding of the influence of the surface parameters on the reflectivity properties.

"Fig. 4 depicts the influence of each functional parameter on the surface reflectivity properties. Surfaces with deep valleys (Svk) yield high reflectivity contrast with peaks (light area) due to the reflected light coming from valleys is blocked, creating a dark area. On the contrary, surfaces where the core roughness (Sk) prevails over all functional parameters, lower reflectivity contrast is expected between valleys and peaks. This is because the blocked light coming from valleys is reduced, leading to higher light area as compared to the dark one."

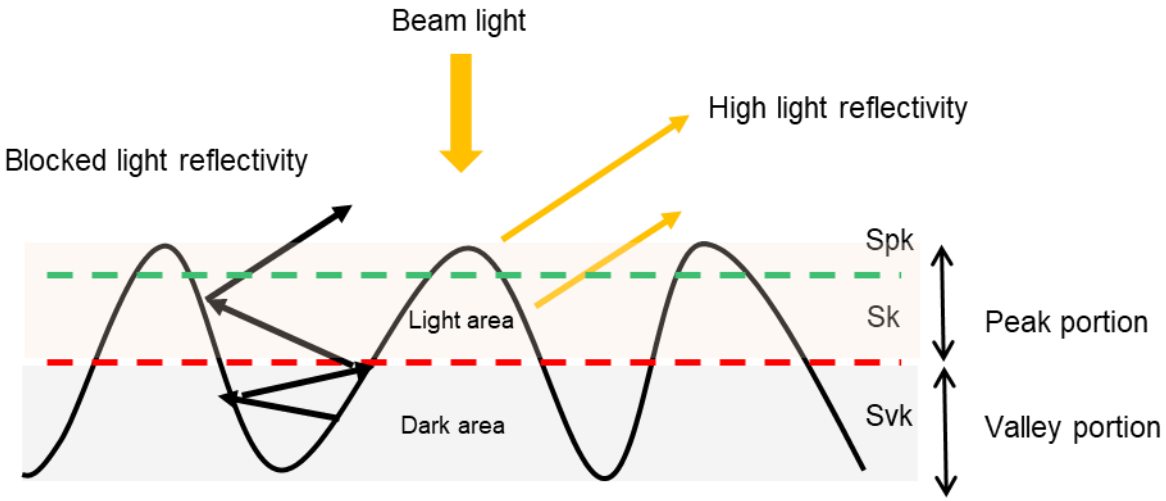

- The citation "Fechner was the first in introducing the word psychophysics and published several studies on perception [2].", you should use the original publication or change the text, as it was descibed by Pelli and Bex ....

  Thank you for your recommendation. The text has been modified as follows:

  "In 1860 Fechner introduced the word psychophysics in his entitled book, Elemente der Psychophysik [Fechner, GT. Elemente der Psychophysik. 1860. Leipzig: Breitkopf und Hertel. In: Adler, HE., editor. Elements of Psychophysics. Holt, Rinehart, and Winston; New York: 1860/1966. 1966]. Consequently, several studies were published on perception [2] which meant the beginning of the modern era in the perception-detection field."

- You should provide some information about the filters used (L, S etc)

  Thank you for your comment. The filters have been described as follows:

  "The S-filter was utilized for removing the short spatial wavelength or small features of the topography. The L-filter was employed to remove the large spatial wavelength (large features) and the F-Operator was used to remove the base form or the geometrical surface component. The combination of these three filters yielded SF or SL surfaces as defined by the standard ISO 25178-2 [37]. The SF-surface was derived by removing the lateral components (surface features) smaller than the selected S-filter and larger than the F-Operator value, whereas the SL-surface was the result of applying the L-filter on the previously defined SF-surface. Filtering by feature size yielded a better topography perceptibility for a given scale, leading to an adequate separation of the three surface components [38]."

- I would change the structure of your paper a bit and describe and define in the experimental part all of your parameters (FHD, TS, TAA) together with the or after the conventional surface roughness parameters used. Than I would describe and discuss the results in the Results chapter. I do not find a proper definition of FHD (mentioned in the Abstract and next in 3.3.1 results ?) you are stating the importance of these parameters in the abstract and in the introduction, a good summary of all definitions would help to understand their importance.

  Thank you for your comment, the paper structure was slightly modified and the definition of the novel parameters introduced were included in the method part as follows:

  "The relationship between the surface topography and its reflectance properties was established through the introduction of four novel parameters. The absolute functional height (AFH), the functional height distribution (FHD), the texture slope (TS) and the texture aperture angle (TAA). The AFH is defined as the sum of the three above described functional parameters (Spk + Sk + Svk). This parameter allows determining the averaged texture depth within the sampling area. The FHD allows determining the relative amount of each functional parameter, providing information about which functional parameter prevail on the overall topography, having textures where peaks predominate over valleys or vice versa. Fig. 4 depicts the influence of each functional parameter on the surface reflectivity properties. Surfaces with deep valleys (Svk) yield high reflectivity contrast with peaks (light area) due to the reflected light coming from valleys is blocked, creating a dark area. On the contrary, surfaces where the core roughness (Sk) prevails over all functional parameters, lower reflectivity contrast is expected between valleys and peaks. This is because the blocked light coming from valleys is reduced, leading to higher light area as compared to the dark one. The TS is described as the angle formed between the grain surface and its horizontal (underlying surface) and the TAA is the angle between two consecutive grain surfaces. Both TS and TAA were measured as shown in Fig. 5. These two parameters helped to understand the importance of valleys on the light reflectivity performance of a given texture."

- On the other hand your are describing in detail Sa, Sq but there are not pointed out in the abstract.

  The parameters Sa and Sq have been pointed out in the abstract as follows:

  "Alternative topographical parameters such as the absolute functional height (AFH), the functional height distribution (FHD), texture slope (TS) or texture aperture angle (TAA) besides to the traditional roughness parameters such as the arithmetical mean height (Sa) and the root mean square height (Sq) have been utilized to characterize the random surface textures."

- I am speculation about the randomness or regularity of your multiscale structures, could you create a combinaed parameter/explanation for providing a scale (from 0 to 1) to the randomness at various scales

  Thank you for your comment and contribution.

  The degree of randomness/isotropy of the surface has been quantified using spatial parameters such as the autocorrelation function (ACF), autocorrelation length (Sal) and the texture aspect ratio (Str). The manuscript has been modified in the materials and methods and results chapters in order to define and discuss these parameters and the obtained results.

Highlights

- An alternative to painting for obtaining high quality surfaces is proposed.
- High quality surfaces can be obtained by applying mould cavity treatments.
- The surface perception can be related to topographical characteristics.
- Texture slope and functional height distribution affect peaks to valleys contrast.
- The reflectivity contrast depends on the amount of deep valleys.

Manuscript File Click here to view linked References

Influence of topographical features on the surface appearance measurement of injection moulded components.

P.Gamonal-Repiso[1,2], T. Abt[1], M.Sánchez-Soto[1], S. Santos-Pinto[2], M. Ll. Maspoch[1].*

[1] Centre Català del Plàstic, Universidad Politécnica de Catalunya Barcelona Tech (UPC-EEBE), C/Colom 114, 08222 Terrassa (Spain).

[2] Departamento de Tecnología de Materiales de SEAT S.A. Autovía A-2, Km 585. Apartado de correos 91. 08760 Martorell, Spain.

*Corresponding author:

E-mail adress: m.sanchez-soto@upc.edu (Miguel Sánchez-Soto);

Influence of topographical features on the surface appearance measurement of injection moulded components.

P.Gamonal-Repiso[1,2], T. Abt[1], M.Sánchez-Soto[1], S. Santos-Pinto[2], M. Ll. Maspoch[1].*

[1] Centre Català del Plàstic, Universidad Politécnica de Catalunya Barcelona Tech (UPC-EEBE), C/Colom 114, 08222 Terrassa (Spain).

[2] Departamento de Tecnología de Materiales de SEAT S.A. Autovía A-2, Km 585. Apartado de correos 91. 08760 Martorell, Spain.

Abstract

Adding textures to surfaces is known to improve the external appearance of injection moulded components. However, when high surface quality is required, normally a paint coating is applied on top of the moulded textured surface. In this work, an alternative to painting for obtaining high quality surfaces is proposed, following an environmental-friendly process and having low production cost. Three different surface textures obtained by injection moulding have been characterized and compared with a painted one. Alternative topographical parameters such as the absolute functional height (AFH), the functional height distribution (FHD), texture slope (TS) or texture aperture angle (TAA) besides to the traditional roughness parameters such as the arithmetical mean height (Sa) and the root mean square height (Sq) have been utilized to characterize the random surface textures. The relationships between these parameters and the surface quality appearance represented by gloss and reflectivity contrast have been established using a new total appearance measurement (TAM) apparatus. It was found that by applying secondary operation on the textured mould cavity, such as adding micro roughness features or coatings, equal apparent quality to the ones obtained by painting can be reached.

Keywords: Injection moulding; Micro roughness; Reflectivity contrast; Surface appearance

*Corresponding Author. Miguel Sánchez-Soto. Mail to: m.sanchez-soto@upc.edu

1. Introduction

The appearance of an object depends on two main characteristics, namely colour and the geometrical attributes of its surface. Colour allows identifying the aspect of an object whereas the geometrical attributes affect gloss and texture. The perception of these characteristics are influenced by both the direction of illumination and view, leading to perceive light varying point by point over a surface with uniform colour [1].

The capability of the human eye to perceive objects under different illumination conditions, surface morphologies or angles of visualization has been of great interest in the field of psychophysics. This science quantifies the relation between physic stimuli and its perception. In 1860 Fechner introduced the word psychophysics in his entitled book, Elemente der Psychophysik [Fechner, GT. Elemente der Psychophysik. 1860. Leipzig: Breitkopf und Hertel. In: Adler, HE., editor. Elements of Psychophysics. Holt, Rinehart, and Winston; New York: 1860/1966. 1966]. Consequently, several studies were published on perception [2] which meant the beginning of the modern era in the perception-detection field.

The detection and perception of an object is accomplished through the human visual system (HVS), which can be divided in two main components: the eyes and the brain. The former is the responsible of capturing light and convert it into signals whereas the latter processes the signals and takes decisions about the viewing of object as perception [3–6]. The contrast is defined as the relative difference in luminance between a target and its background and is used to determine what is detectable by the HVS. Objects are visible if they posses a contrast larger than the contrast sensitivity (CS) [6–13]. Sukumar et al. [6] analysed the perception-detection threshold of an object by varying the contrast as a function of the illumination conditions. The contrast sensitivity function (CSF), which was introduced by Campbell and Robson [12] was used in this analysis, founding that changes in visibility, acuity and colour perception were altered with the illumination conditions. Pelli and Bex [2] reviewed the methodologies for estimating the contrast sensitivity threshold. Methodologies such as one trial, trial sequence or

the CSF were analysed, finding that the multiple-alternative forced-choice detection methodology (trial sequence) was the most reliable, reducing subjectivity and guessing rate of the observers, thus being the more informative methodology.

On the other hand, beyond establishing thresholds to the HVS through the CSF, the influence of the interaction of surface properties such as gloss and texture on the perception has been also object of research [17-30]. Obein et al. [14] studied the correlation between the gloss scales of black coated samples with the judgements of observers using two illumination directions. The results showed a nonlinear relation between the gloss level and its perception, having higher sensitivity in the extreme values of gloss rather than in the middle ones. Ho et al. [27] studied the interaction between texture and gloss by using the judgments of observers and modelling how each of these properties affect perception. It was found that observers perceived rougher surfaces with high gloss and glossier surfaces with high roughness level, making possible the quantification of its interaction. The degree of influence of texture over gloss was of about 11% whereas the influence of gloss on the roughness perception was of about 27%. Fleming et al. [17] made a reflectance matching task for accurately estimate the surface reflectance detected by the human eye. The results demonstrated that surface reflectance properties such as lightness and gloss matched well under realistic lighting conditions. The opposite result was obtained using modified illumination conditions that were not representative of the real world. It was concluded that the human brain stored assumptions about real-world illumination conditions for estimating surface reflectance. Schmid and Anderson [20] made a series of experiments for studying the influence of both the reflectance properties and the surface micro roughness on the perceived lightness. It was found that the lightness constancy was better for those surfaces with higher gloss and visible mesostructure (micro roughness) than the matte ones.

All of the above described valuable studies define how the HVS works and they have developed methodologies to determine new thresholds to the human eye under different illumination and viewing conditions. However, it is necessary to quantify these judgements and translate them

into numerical measurements. Colour and gloss can be measured using colorimeters and glossmeters, respectively. On the contrary, surface appearance is not yet directly measurable and depends on visual judgments. This leads to establish a new methodology that allows measuring the surface appearance objectively regardless of the visual evaluations. It would be helpful for the evaluation of textured interior trims, for instance in the automotive industry, where its surface appearance is strongly related to the customer's quality perception.

Nowadays, the car cabin is not just a place for driving, it is considered as a "living space" where the driver and passengers should be comfortable and surrounded by a harmonious environment. Processes such as leather-line, chromed or painted have been used to modify the surface appearance in order to reach the desirable quality feeling inside the car. On the other hand, the main drawback of these technologies is their high cost-production which limits its implementation to luxury car models and the lack of environmental-friendly processes. Alternatively, injection moulding of decor trims has become a cost competitive manufacturing process. Problems with gloss and non-uniformity are commonly encountered and the surface finish is perceived as low quality. To solve this, surface texturing became in an appealing solution for enhancing the surface quality, leading to design textures that mimic materials such as leather, wood or metal, among others [28–34].

This paper seeks to obtain objective measurements of the surface appearance of objects. The use of a novel total appearance measurement instrument (TAM) is proposed to adequately and objectively determine the surface appearance of randomly micro-textured injection-moulded surfaces. New topographical parameters such as texture slope (TS) and texture aperture angle (TAA) were introduced to establish relations between surface topography and its appearance. In addition, multi-scale analysis [35,36] or surface image analysis characterization techniques were employed in this work.

2. Material and methods

2.1 Materials and processes

An Engel Victory 110 injection moulding machine (Engel Austria GmbH) equipped with a screw of 40 mm diameter was used to mould squared samples with dimensions of 100 x 100 x 3 mm^3. In all cases a black polypropylene copolymer filled with 5% talc was used, namely HC TKC 2007N from Basell S.L (Tarragona, Spain). It was characterised by a melt flow index of 16 g/10min (ISO 1133, 230 ºC, 2.16 kg) and an ethylene content of about 8 wt.%. The injection conditions were as follows: melt temperature = 235 ºC, mould temperature = 50 ºC, injection speed = 300 cm^3/s, holding pressure = 600 bar. According to a previous research these were the most suitable injection moulding conditions [35]

A leather texture type with a random design was used for studying the surface quality as a function of the topographical features. This texture was obtained through a chemical engraving process that consisted in printing the leather texture on the mould cavity by using an acid-resistant ink. After immersing the cavity several times in an acid bath, the desired texture depth was obtained. This initial texture was coded as Texture A. The texture finish was then slightly modified by applying two different secondary operations defining Textures B and C. Texture B was obtained following the above described procedure but including an extra step which added micro-features on top of the surface. Texture C was obtained after uniformly applying a mixture of polytetrafluoroethylene and graphite on the engraved mould cavity and allowing it to cure in an oven at 350 ±10ºC.For comparison, a painted surface (Texture D) was created as follows. A black water-based paint from Mankiewicz Iberica S.L (Barcelona, Spain) was applied on top of Texture A injection moulded samples. This procedure was performed manually in a standardized painting room with controlled temperature of 23 ± 0.5 ºC. As a result, four different surface finishes were obtained as shown in Fig. 1.

2.2. Surface characterization

2.2.1 Surface topography

The topographies of the different surfaces were analysed using a non-contact chromatic confocal microscope, FRT Microprof 200 (Bergisch Gladbach,Germany) that employs a light-emitting diode as source. Its chromatic white light sensor (CWL) had a lateral and vertical resolution of 6 µm and 30 nm, respectively. The data processing was performed using the software FRT Mark III V3.11.5.2.

The topographies were analysed both at the macro- and micro scale. For the macro scale case, the area under analysis was 14.65 x 14.65 mm^2 with a lateral resolution of 40 µm. The analysis at the micro scale was conducted on a 3.65 x 3.65 mm^2 area and using 10 µm of lateral resolution. Filters such as S-filter, L-filter and F-Operator govern the limited scales of the surface. The S-filter was utilized for removing the short spatial wavelength or small features of the topography. The L-filter was employed to remove the large spatial wavelength (large features) and the F-Operator was used to remove the base form or the geometrical surface component. The combination of these three filters yielded SF or SL surfaces as defined by the standard ISO 25178-2 [37]. The SF-surface was derived by removing the lateral components (surface features) smaller than the selected S-filter and larger than the F-Operator value, whereas the SL-surface was the result of applying the L-filter on the previously defined SF-surface. Filtering by feature size yielded a better topography perceptibility for a given scale, leading to an adequate separation of the three surface components [38].

In the macro scale case, both S-Filter and L-Filter were fixed at 0.04 mm and 5 mm, respectively. In addition, a multi scale analysis was conducted at the micro scale [35]. The S-Filter was fixed at 0.01 mm and the L-Filter was varied from 0.025 to 0.2 mm. Thus, the surface analysis was carried out at the limited scales S-L 0.04-5 and S-L 0.01- 0.05. The S-L denotes the surface type, 0.04 mm is the S-filter setting and 5 mm is the L-filter value.

For accurately characterizing the different topographies, parameters from the amplitude, functional and spatial families were considered. From the amplitude parameter family, the arithmetical mean height (Sa) and the root mean square height (Sq) were selected. They are defined by Eq.1 and 2, respectively. Both represent the overall surface roughness but are insensitive in differentiating peaks and valleys.

$$Sa = \frac{1}{A}\iint_A |z(x,y)|dxdy \qquad (1)$$

$$Sq = \sqrt{\frac{1}{A}\iint_A |z^2(x,y)|dxdy} \qquad (2)$$

From the functional parameter family, the core height (Sk), the reduced peak height (Spk) and the reduced dale height (Svk) were taken into account. They were obtained from the areal material ratio curve also known as the Abbot Firestone curve, which is established by evaluating the material ratio at various levels from the highest peak to the lowest valley. Sk represents the core roughness or the averaged peak to valley height. The Spk represents the height above Sk, hence it can be considered as representative of aberrant high peaks. Finally, Svk is the height under Sk, representing the aberrant deep valleys. Fig. 2 depicts the different functional parameters employed.

The autocorrelation function (ACF), the texture aspect ratio (Str) and the autocorrelation length (Sal) were selected from the spatial parameters family. They were used to quantify the degree of isotropy of the textures. The ACF is described by the following equation (Eq. 3) [38]

$$ACF\ (\tau_x, \tau_y) = \frac{\iint_A Z(x,y)Z(x-\tau_x, y-\tau_y)dxdy}{\iint_A Z^2(x,y)dxdy} \qquad (3)$$

Where Z(x,y) is the measured surface, $Z(x-\tau_x, y-\tau_y)$ is a duplicate surface with a lateral displacement (τ_x, τ_y) and $Z^2(x,y)$ is the variance which is employed as normalising factor.

Therefore, the ACF is a measure of how similar the texture is at a given distance from the original location. This function allows obtaining an image with a central peak from which the degree of isotropy of the surface can be quantified. This central peak is the result of normalizing the surface height distribution with the variance ($Z^2(x,y)$). The texture aspect ratio (Str) is used as indicator of the surface isotropy. Spatial isotropic textures will have a Str value close to 1 while anisotropic spatial textures will have a Str close to 0. Finally, the autocorrelation length (Sal) is defined as the minimum distance over the surface so that the new location will have the minimal correlation with the original one.

Fig. 3 shows a graphical representation of the procedure to calculate Str and Sal parameters. The 3D reconstruction of texture A corresponds to the Fig. 3a. The resultant image after applying the ACF with the peak in the centre is shown in Fig. 3b. Finally, Fig. 3c shows the measurement of the maximum and minimum radii of the peak base. In the latter figure, the original peak has been removed from the surface using a threshold that assures that the central lobe edges are well defined. Thus, the Str is defined as the ratio between the length of fastest decay of ACF in any direction (R_{min}) and the length of slowest decay of ACF in any direction (R_{max}) (Eq. 4). The Sal corresponds to the minimum radii (R_{min}).

$$Str = \frac{R_{min}}{R_{max}} \quad (4)$$

Where R_{min} is the minimum radii and the R_{max} is the maximum radii of the resultant base lobe.

A surface with the same characteristics in every direction will present an approximately circular base lobe, resulting in almost the same minimum and maximum radii. On the contrary, in surfaces with strong privileged orientation, the central lobe will present a great difference between the maximum and minimum radii, obtaining an elliptic form of the base lobe.

The relationship between the surface topography and its reflectance properties was established through the introduction of four novel parameters. The absolute functional height (AFH), the functional height distribution (FHD), the texture slope (TS) and the texture aperture angle

(TAA). The AFH is defined as the sum of the three above described functional parameters (Spk + Sk + Svk). This parameter allows determining the averaged texture depth within the sampling area. The FHD allows determining the relative amount of each functional parameter, providing information about which functional parameter prevail on the overall topography, having textures where peaks predominate over valleys or vice versa. Fig. 4 depicts the influence of each functional parameter on the surface reflectivity properties. Surfaces with deep valleys (Svk) yield high reflectivity contrast with peaks (light area) due to the reflected light coming from valleys is blocked, creating a dark area. On the contrary, surfaces where the core roughness (Sk) prevails over all functional parameters, lower reflectivity contrast is expected between valleys and peaks. This is because the blocked light coming from valleys is reduced, leading to higher light area as compared to the dark one. The TS is described as the angle formed between the grain surface and its horizontal (underlying surface) and the TAA is the angle between two consecutive grain surfaces. Both TS and TAA were measured as shown in Fig. 5. These two parameters helped to understand the importance of valleys on the light reflectivity performance of a given texture.

Finally, alternative surface parameters such as the number of cells (NG) within the sampling area and the average hill area ($\overline{GA}$) were considered as reference for adequately setting the TAM prototype instrument to each texture finish [35].

2.2.2 Surface appearance measurement

The surface appearance was measured using a total appearance measurement instrument (TAM) from BYK-Gardner GmbH (Geretsried, Germany). This device was a prototype that enables analysing at the same time surface topography and reflectivity by means of the photometric stereo technology (PS) [39]. This technique allows making surface reconstruction in three dimensions (3D) through successive images by varying the direction of the incident illumination but keeping constant the scene and the viewing direction (Fig. 6). For this reason, the prototype instrument incorporates four white tri-phosphor-LEDs as light source, each one

at 60º in regards to the horizontal axis. A top camera, equipped with tele-centric lenses is located at 0º with respect to the surface normal.

For measuring the reflectivity the prototype assumes the surface as Lambertian or ideal diffusion type [40]. These Lambertian surfaces are characterized by having equalbrightness in any viewing direction at a fixed light source. However, the intensity of the surface image changes if the illumination directions are modified. Thus, reflectivity measurements were carried out using a top light source located at 0º with respect to the surface normal. The evaluation area was approximately 15 x 15 mm^2, taking 512 x 512 pixels per image which resulted in an optical resolution of around 60 µm. This mimics a human visual angle of 0.11º at a distance of 300 mm [41]. The surface gloss (G*) was measured using a spectro-Guide 45/0 Gloss-spectrophotometer from BYK-Gardner GmbH (Geretsried, Germany). It was equipped with a 45/0º measuring geometry and D65/10º as illuminant. The gloss measurements were acquired at 60º and relative to a highly polished black glass standard with 100 gloss units (GU).

3. Results and discussion

3.1 TAM uncertainty measurements

The procedure described by Haitjema et al. [42] was utilized for determining the uncertainty of the TAM prototype measurements. This methodology allowed estimating the instrument uncertainty by performing repeated measurements on a calibrated item [43]. In this case, Texture A was employed as calibrated item. The number of cells detected within the evaluated area, the mean reflectivity, the reflectivity contrast and the mean hill size were selected as representative parameters for estimating TAM uncertainty (U_{TAM}) according to Eq. 5.

$$U_{TAM} = \sqrt{U_{cal}^2 + U_p^2 + U_{res,TAM}^2} \quad (5)$$

Where U_{cal} is the standard deviation of 10 measurements performed on different locations of the sample. U_p is the standard deviation of 10 repeated measurements performed at the same location and U_{resTAM} is the resolution uncertainty related to the declared 60 µm optical resolution of the TAM instrument, which it is equal to 0.03. All the measurements were performed in a temperature-controlled room at 23 ± 1 ºC.

The different sources of uncertainty are collected in Table 1. It is noted that the highest source of uncertainty was due to the deviation of the Texture A itself (U_{cal}). This was because its random nature mimicking leather did not follow any regular pattern or sequence. In the case of the measuring deviation (Up) the obtained values were almost zero. Therefore, it was concluded that the measurements of the TAM instrument were reliable and repeatable.

Table 1.

Uncertainty contribution to the TAM prototype instrument.

Uncertainty contribution	Nº cells	Mean reflectivity (a. u)	Reflectivity contrast	Mean hill size (mm^2)
U_{cal}	166 ± 11	186 ± 7	0.24 ± 0.01	0.72 ± 0.04
U_p	160 ± 0.4	193 ± 0.4	0.23 ± 0.03	0.74 ± 0.01
U_{TAM}	11.0	7.0	0.04	0.05

3.2 TAM settings as a function of the texture topography

Once the uncertainty contribution of the prototype instrument was established, the next step before characterizing any surface was to perform a comparison with a known technique. The chromatic confocal microscope was selected as a reliable and suitable method for characterizing surface topographies. The measurements obtained with the chromatic confocal microscope were used for reaching the adequate settings of the TAM prototype for each surface finish.

The surfaces under study were first measured with the CWL sensor under the previously described measuring conditions at five different locations (Fig. 7). Table 2 collects the results of the number of cells (NG), the mean hill area ($\overline{GA}$), the absolute functional height (AFH) and its relative portion of deep valleys (Svk) obtained using the CWL sensor.

Table 2
Topographic results of each texture finish measured with the CWL sensor and took as reference for TAM setting.

	NG	$\overline{GA}$ (mm^2)	AFH (µm)	Svk (%)
Texture A	174 ± 6	0.72 ± 0.03	107 ± 2	43.4 ± 1.7
Texture B	258 ± 8	0.46 ± 0.01	90 ± 2	26.7 ± 1.2
Texture C	227 ± 5	0.51 ± 0.01	87 ± 1	26.0 ± 0.8
Texture D	145 ± 13	0.81 ± 0.08	72 ± 2	25.9 ± 2.6

The TAM prototype had different filters for adequately measuring the topography of a surface and its reflectivity properties. These filters are the offset, plateau offset, the reflectivity contrast threshold (RCT) and the hill size threshold (HST). The filter and plateau offset control the smoothing of the input data and the truncation of the crest of peaks, respectively. They directly affect the watershed algorithm, which detects the number of cells within the evaluated area as shown in Fig. 8. Fig. 8a corresponds to the obtained topography with a filter offset value of 5, resulting in 47 detected cells. On the contrary, Fig. 8b shows the same evaluated area setting the filter offset to 50, which resulted in 302 cells. Therefore, the number of cells (NG) detected by the CWL sensor was used as reference to adequately set the filter offset and avoiding over- or undersegmentation.

The RCT and the HST control the segmentation of hills and valleys, measuring the reflectivity contrast and the hill size, respectively. The filter ranges from -1 to 1, where – 1 means that the lowest point of the topography is used as threshold, hence 100% of data is selected as peak. The value +1 leads to the reverse output. It should be pointed out that the RCT filter takes into account relative values to differentiate peaks from valley portions throughout the entire topography. For this reason, the relative amount of deep valleys (% Svk) was used as reference to set this filter. Finally, the $\overline{GA}$ measured was used to properly set the HST filter of the TAM

prototype instrument. As said before, all these measurements were first obtained with the CWL sensor to calibrate the TAM prototype.

The obtained setting and results of TAM prototype instrument are shown in Table 3. It should be remarked that the texture types with higher number of cells (Texture B and Texture C) exhibited as well higher filter offset values. This means that, for the same evaluated area (15 mm^2), the higher the number of detected cells the finer is the topographic mesh obtained by the watershed algorithm. In addition, it matches well with the fact that the resultant $\overline{GA}$ of both Texture B and Texture C were smaller having 0.46 and 0.51 mm^2, respectively. As shown in Table 2, texture A was the one showing a different RCT filter value (-0.1) in comparison to the rest of analysed surfaces (-0.5). This was because Texture A had the highest relative amount of deep valleys in its topography, accounting for 43% of the total, whereas for the other textures it was 26% in average. On the other hand, the HST filter was set through trial-error approach using the CWL data as reference (Table 2).

Table 3.

Settings and topographical results obtained with TAM prototype.

	TAM's setting			TAM's results	
	Filter offset	RCT	HST	NG	$\overline{GA}$ (mm^2)
Texture A	20	-0.1	-0.2	164 ± 8	0.73 ± 0.03
Texture B	30	-0.5	-0.1	243 ± 9	0.44 ± 0.02
Texture C	25	-0.5	-0.2	217 ± 5	0.53 ± 0.02
Texture D	20	-0.5	-0.2	149 ± 6	0.77 ± 0.03

As shown in Table 2 and Table 3, the obtained results of NG and $\overline{GA}$ by both CWL sensor and TAM instrument were within the deviation range. Hence, it can be assumed that the settings of TAM were adequately selected for each of the texture finish types.

The proper setting of the TAM instrument is of prime importance because this novel equipment allows to quantify the reflected light coming from both peaks and valleys, resulting in a contrast based on the Michelson equation (Eq. 4) [2,5].

$$C = \frac{R_{peak} - R_{valley}}{R_{peak} + R_{valley}} \quad (4)$$

Where C is the reflectivity contrast, R_{peak} is the reflectivity on the peaks portion and R_{valley} is the reflectivity in the valleys portion. The contrast sensitivity criteria was established at 2% [5]. When the reflectivity contrast is larger than this value it is expected that peaks can be distinguished from the valleys background. In the present case, deep valleys (Svk) were selected as surface background, since this surface portion was less illuminated. Therefore, the appearance of the surface can be measured in terms of the reflectivity contrast between peaks and valleys. It can be related with objective data such as %Svk, NG or AFH, coming from the measurement of the surface topography.

3.3 Topographical characterization.

3.3.1 Measurement of the surface isotropy

The four engraved textured surfaces under study were analysed for determining its degree of isotropy. It was quantified at the S-L 0.04-5 scale with 40 µm of lateral resolution. Table 4 collects the results of the R_{min}/Sal, R_{max} and Str. As it can be seen, the degree of isotropy is higher than 0.70, resulting in surfaces without any preferential orientations. Therefore, it can be said that the textures under study are random surfaces, since they do not follow any defined pattern or sequence. In addition, the R_{min} and Sal value provide an indication of the spectral content of the surface. A high Sal value implies high amount of long wavelength components.

Therefore, it can be expected a higher level of micro roughness in Textures A, B and C in comparison to Texture D.

Table 4.

Isotropy results of the four textures under study at the macro-scale.

S-L 0.04-5	R_{min} / Sal (mm)	R_{max} (mm)	Str
Texture A	0.36	0.50	0.72
Texture B	0.36	0.44	0.82
Texture C	0.36	0.48	0.75
Texture D	0.46	0.62	0.74

3.3.2 Macro scale analysis

The three injection moulded samples (Texture A, B and C) were compared with the painted one (Texture D) in terms of topographical features and surface reflectivity contrast to determine the feasibility of obtaining unpainted engraved surfaces having similar appearance than the painted one. The relationship between surface characteristics such as roughness, functional distribution heights (FDH), texture slope (TS) and texture aperture angle (TAA) with the surface reflectance properties (reflectivity contrast) were studied for quantitatively measuring the surface appearance. The two parameters TS and TAA are of great importance in order to understand the role of valleys in the light reflectivity of the textured surface (Eq. 6). As described in Eq. (6), in a Lambertian surface the intensity of the light reflected depends on the angle between the incident beam light and the surface normal [40,44].

$$E_\theta = E\cos\Theta \qquad (6)$$

Where E_Θ is the light intensity, E is the maximum light intensity at 0º in regards to the surface normal and Θ is the angle of incidence between the light source and the surface normal.

Therefore, in the case of the TS, the closer the angle to 90º the lower the reflectivity from valleys portion is expected. In the TAA case, the lower the angle between grains walls the lower will be the reflected light coming from valleys.

Table 5 contains the topographic results obtained at the limited scale of S-L 0.04-5 of the textures under study. It should be pointed out that in comparison to the other textures, In comparison to the other textures, texture A exhibited in average the highest roughness values of Sa and Sq and the highest AFH with a total of 107 µm (Spk + Sk + Svk). However, it should be pointed out that the FHD was different between textures. Texture A had a FHD of Spk, Sk and Svk of 3%, 53% and 43%, respectively. This means that from the total topography, 3% pertains to aberrant peaks, 53% to peak-to-valley height and 43% to aberrant deep valleys, which were selected as surface background to adequately measure the reflectivity contrast between peaks and valleys. Texture A had the lowest Spk value, which indicated low roughness level on top of the surface, leading to specular reflections. Therefore, high reflectivity contrast can be expected because of the apparition of dark areas coming from valleys portion and specular reflections coming from the top of peaks. Textures B, C and D exhibited similar ranges of FHD in their topographies with 6.0%, 67.7% and 26.2% of Spk, Sk and Svk in average. In these cases, their FHD lead to expect less reflectivity contrast between top surface and its background. This is because when the amount of peaks (i.e. Spk) is high, the diffuse light component prevails over the specular one. In addition, due to the low amount of deep valleys (i.e. Svk) in their topographies, smaller dark areas coming from deep valleys portion are expected. Another parameter to take into account is the relative core roughness height (Sk). This surface portion represents the peak-to-valley height and it is homogeneously illuminated, as described in a previous work [45].

Table 5

Topographic results at the limited scale S-L 0.04 – 5.

	Sa (µm)	Sq (µm)	AFH (µm)	Spk (%)	Sk (%)	Svk (%)
Texture A	25.4 ± 0.4	30.0 ± 0.5	107 ± 2	3.3 ± 0.5	53.3 ± 1.3	43.4 ± 1.7
Texture B	21.6 ± 0.7	25.0 ± 0.9	90 ± 2	6.6 ± 1.1	66.6 ± 0.9	26.7 ± 1.2
Texture C	22.4 ± 0.4	25.4 ± 0.5	87 ± 1	4.9 ± 1.0	69.1 ± 0.7	26.0 ± 0.8
Texture D	15.9 ± 0.8	18.8 ± 1.0	72 ± 2	6.6 ± 1.0	67.5 ± 2.4	25.9 ± 2.6

3.3.3 Micro scale analysis

The textures were also analysed at the micro scale. Fig. 9a and 9b show the values of Sa and Sq at each limited scale. As can be appreciated, at the lower limited scales (L-Filter of 0.025 and 0.05 mm), the Texture C showed relatively higher roughness values in both Sa and Sq. On the other hand, when the evaluation scale (L-filter) was increased to 0.2 mm, Texture B was the one exhibiting higher roughness values. The secondary operations during the mould engraving such as the addition of micro roughness and the mould coating modified the underlying Texture A (Fig. 10a). In the former case (Texture B), the micro-asperities included during the engraving process were of approximately 200 µm in the lateral dimension (x, y) as shown in Fig. 10b. In the latest case (Texture C), the applied coating induced micro-asperities ranged from 25 to 50 µm (Fig. 10c) while the painted surface (Texture D) had the lowest micro roughness values at all scales that ranges from 0.6 to 1.4 µm in Sa for 0.025 and 0.2 mm of L-filter, respectively. This indicates that the painting process smoothed the original texture, reducing both top micro-asperities on peaks and deep valleys by filling the gaps as illustrated in Fig. 10d. It should be remarked that the gloss of each texture finish (Table 6) matched well with its obtained roughness level at the micro scale (Fig. 9a and 9b). High surface micro roughness implies low gloss level. The reason behind this behaviour is that the surface gloss is mainly controlled by

the diffuse component of the reflected light. In addition, the gloss measurement were done at 60º, having as main source of reflected light the one coming from peaks portion. Valleys have no contribution to the surface gloss measurement. The reflected light coming from valleys is blocked by the surface peaks and does not enter into the glossmeter's detector. However, the surface appearance does not only depend on peaks portion and its gloss. The human eyes can visualize the total surface, taking into account both the light reflected from peaks and from valleys. As well, the TAM prototype instrument allows quantifying the light reflected from peaks and valleys, measuring the reflectivity contrast objectively.

Table 6

Results of gloss measurements at 60º.

	Texture A	Texture B	Texture C	Texture D
Gloss (GU)	1.7 ± 0.1	1.2 ± 0.1	1.3 ± 0.1	1.9 ± 0.1

3.4 Surface appearance measurement

The quality of a certain surface is mainly dependent on its gloss, colour and texture [26,28,29,46]. For instance, in cosmetics industry smooth and glossy surfaces are preferred to provide high quality to their customers. On the contrary, in automotive, high quality surface is achieved with matte finishes. In this case, gloss level lower than 2.0 GU at 60º is preferred because it provides a better surface appearance to the customers. Texturing is a common employed technique to reach the desired quality, although painting textured surfaces provides the best quality and appearance finish in automotive sector.

In the present case, the painted texture (Texture D) was selected as reference of high quality surface appearance. Hence, textures A, B and C, obtained directly from the mould cavity, were then compared to texture D. The aim was to determine if injection moulded components can achieve reflectivity properties that allow reaching similar quality appearance than the painted one.

Fig. 11 shows the reflectivity values coming from peaks and valleys for all texture types. It can be appreciated that texture A had by far the higher reflectivity coming from peaks. Moreover, Texture A exhibited the highest difference between the light reflected from peaks and valleys, resulting in the highest contrast with a value of 24% ± 2. On the contrary, both texture B and texture C had a more balanced reflectivity from peaks and valleys. This leads to a low reflectivity contrast with 3% ± 1 and 0% ± 3 for texture B and C, respectively. Finally, texture D presented negative reflectivity contrast between peaks and valleys with – 6% ± 1. This was attributed to the amount of reflected light coming from valleys was higher than the one coming from peaks.

The above described behaviour can be related to the topographical features of each particular texture type. As previously mentioned, the amount of deep valleys (i.e. %Svk) was selected as surface background. It is shown in Fig. 12, where the reflectivity maps of the different texture types are shown. The black area of the figure corresponds to deep valleys portion (background) and the illuminated one to the peaks portion. Texture A had 43% of deep valleys in its total topography (Fig. 12a), which was the one with the lowest amount of reflected light coming from this surface portion. In addition, the low level of micro roughness on top of peaks led to specular reflections, resulting in the highest reflectivity contrast. On the contrary, textures B and C (Fig. 12b and 12c, respectively) with 26% of deep valleys contained in their topographies exhibited a higher amount of light reflected from valleys. In both cases the amount of light reflected from peaks was the lowest one. This last factor correlated well with their high amount of micro roughness on top of the peaks. Finally, texture D (Fig. 12d) had a similar amount of deep valleys (26%) as compared to textures B and C. However, it exhibited the highest amount of reflected light coming from valleys, resulting in a negative reflectivity contrast. This can be explained through the two proposed novel parameters, TS and TAA.

Unlike glossmeter instruments, the human eyes capture light coming from the entire surface, taking into account both peaks and valleys. For this reason, the TAM prototype instrument,

which considers the reflected light coming from peaks and valleys, provides a measurement of appearance closer to the one of human eyes. From the topographical point of view, measuring TS and TAA provides a forecaster about the amount of reflected light coming from valleys of each texture type. As described by Eq. 5, the light intensity in a particular direction is proportional to the cosine of the reflected angle. In the present case, the light source was located at 0º in regards to the surface normal, hence the light reflected in the same direction yielded 100% of intensity. On the contrary, by increasing the reflected angle the intensity of the reflected light decreased. The valleys contribution to the reflectance properties of a textured surface such as the reflectivity contrast depends on the TS and TAA. Combining it with the micro roughness level of peaks, the reflectivity contrast between peaks and valleys can be estimated. Table 7 collects the TS and the TAA averaged results after 20 measurements done at different locations of each texture type.

Table 7

Results of the texture slope (TS) and texture aperture angle (TAA) of the four texture finishes.

	Texture A	Texture B	Texture C	Texture D
TS (degree)	19.4 ± 6.8	15.2 ± 7.3	13.8 ± 4.9	8.2 ± 1.7
TAA (degree)	140.7 ± 11.4	149.6 ± 13.1	152.4 ± 5.3	164.9 ± 2.9

Texture A had the highest TS and therefore yielded the lowest TAA. Hence, the low reflectivity in valleys matched well with the described Lambertian surface. The higher the surface TS the closer to 90º degrees is the angle between the reflected light and the light source, resulting in low light reflectivity. In addition, topographical features such as the relative amount of deep valleys (%Svk) yielded low level of reflected light coming from this surface portion. This texture design blocked light coming from valleys and it did not allow illuminating the surface uniformly. As a consequence, a high reflectivity contrast between peaks and valleys was obtained (24%). On the other hand, textures B and C had less acute TS, resulting in a higher

TAA. This led to a more uniform illumination of the total surface. Unlike texture A, the design of textures B and C allowed the reflected light that came from valleys to be quantified by the TAM prototype instrument, reducing light blocking by peaks. Combining it with their micro roughness level on peaks a less reflectivity contrast can be obtained, having 3% and 0% in texture B and C, respectively. For the case of texture D, the lowest TS and the highest TAA values were found, resulting in even higher reflectivity in valleys than in peaks as it is shown in Fig. 11. It can be concluded that by modifying the underlying design textures that do not block light from peaks portion and yield similar surface appearance to the painted surface can be obtained directly by injection moulding. Therefore, applying surface treatments to the mould cavity is an appealing method for enhancing the surface appearance of injection moulded components, avoiding the high cost and environmental impact of painted surfaces.

4. Conclusions

In this work a texture mimicking leather (texture A), was modified by different secondary operations such as the addition of micro-asperities (texture B), mould coating (texture C) or painting (texture D). The main purpose was to obtain injection moulded surfaces having similar appearance than the painted one, reducing in this way costs and obtaining a more environmental friendly process.

The relationship between the topographic features such as roughness, functional height distribution (FHD), texture slope (TS) and texture aperture angle (TAA) with the surface appearance properties such as gloss and reflectivity have been established. The gloss level of the surfaces was controlled by the micro roughness located on peaks. Texture A had the higher roughness level in the macro scale (S-L 0.04-5) but its surface gloss was not the lowest one (1.7 GU at 60º). Both textures B and C having lower roughness values at the macro scale had lower gloss results. This was because their roughness value at the micro scale (S-L 0.01-0.05 and S-L 0.01-0.2) were the larger ones, resulting in lower gloss 1.2 and 1.3 GU at 60º, respectively.

The contribution of valleys in the surface reflectance properties and thus in its appearance was considered for better understanding of surface perception in terms of reflectivity contrast. It was demonstrated that the functional height distribution (FHD) plays an important role in the reflectivity contrast of the surfaces. The larger the amount of deep valleys (Svk) the larger was the reflectivity contrast reached. The angle of incidence between the light beam and the surface normal was the main responsible of the reflectivity values in valleys portion. The TS and TAA measurements showed that the texture A, with the sharpest TS and thus the closer TAA, was the one with lower reflectivity in valleys, resulting in higher contrast values between peaks and valleys. On the contrary, textures B and C had values of TS and TAA closer to the ones measured on texture D (painted), resulted in turn in similar values of contrast.

Finally, it can be concluded that it is possible to achieve similar surface reflectance properties to the ones obtained by painting. Mould treatments can be an appealing methodology for obtaining surfaces with a high quality aspect ratio at lower cost-production and using an environmental friendly process.

5. Acknowledgements

The authors would like to thank the Ministry of Economy and Competitiveness of the Spanish Government for financially supporting this work through the project MAT201680045-R (AEI/FEDER, UE). Standex International S.A is acknowledged for engraving the texture on the mould cavity and Lyondell Basell S.L for providing the polymer used in this research. BYK-Gardner is acknowledged for providing the Total Appearance Measurement instrument in the final prototyping version.

Data Availability

The raw/processed data required to reproduce these findings cannot be shared at this time as the data also forms part of an ongoing study.

Nomenclature

3D	three-dimensional	R_{max}	maximum radii
AFH	absolute functional height	R_{min}	minimum radii
ACF	Autocorrelation function	Sa	arithmetical mean height
C	contrast	Sal	autocorrelation length
CS	contrast sensitivity	Sk	core height
CSF	contrast sensitivity function	Spk	reduced peak height
FHD	functional height distribution	Sq	root mean square height
HST	hill size threshold	Str	texture aspect ratio
HVS	human vision system	Svk	reduced dale height
PS	photometric stereo	Ucal	Uncertainty of the calibrated surface
RCT	reflectivity contrast threshold	U_{TAM}	Uncertainty of the measurand
TAA	texture aperture angle	Up	Uncertainty of the measurement
TAM	total appearance measurement	$Ures,_{TAM}$	Uncertainty of the camera resolution
TS	texture slope		

6. References

[1] R. S Hunter and R. W. Harold, The Measurement of Appearance, Wiley, USA (1987).

[2] D.G. Pelli, P. Bex, Measuring contrast sensitivity, Vision Res. 90 (2013) 10–14. https://doi.org/10.1016/j.visres.2013.04.015.

[3] P. Barten, Contrast sensitivity of the human eye and its effects on image quality, 1999. https://doi.org/10.1117/3.353254.

[4] De Valois, R.L, De Valois, K.K., Spatial vision, 4th ed. New York: Oxford University Press; 1988.

[5] A. Michelson. Studies in optics. U. of Chicago Press, 1927.

[6] V. SUKUMAR, H.L. HESS, K. V. NOREN, G. DONOHOE, S. AY, Study on Threshold Patterns with Varying Illumination Using 1.3m Imaging System, Intell. Inf. Manag. 02 (2010) 21–25. https://doi.org/10.4236/iim.2010.21003.

[7] B. Pelli, D.G., and Farell, Why use noise?, J. Opt. Soc. Am. A, Opt. Image Sci. Vis. 16 (1999) 647. https://doi.org/10.1364/JOSAA.16.000647.

[8] F. Hou, L.A. Lesmes, W. Kim, H. Gu, M.A. Pitt, J.I. Myung, Z.-L. Lu, Evaluating the performance of the quick CSF method in detecting contrast sensitivity function changes, J. Vis. 16 (2016) 18. https://doi.org/10.1167/16.6.18.

[9] P.J. Bex, W. Makous, of Natural Images, America (NY). 19 (2002) 1096–1106.

[10] C. Marois, D. Lafreniere, B. Macintosh, R. Doyon, Confidence Level and Sensitivity Limits in High-Contrast Imaging, Astrophys. J. 673 (2008) 647–656. https://doi.org/10.1086/523839.

[11] B. Watson, Visual detection of spatial contrast patterns: evaluation of five simple models., Opt. Express. 6 (2000) 12–33. https://doi.org/10.1364/OE.6.000012.

[12] T.J. Rink, R.Y. Tsien, Application fo fourier analysis to the visibility of gratings, 50 (1981) 531–548.

[13] J.J. Koenderink, A.J. Van Doorn, Illuminance texture due to surface mesostructure, 13 (1996) 452–463.

[14] G. Obein, F. Viénot, U. Claude, B. Lyon, Difference scaling of gloss : Nonlinearity , binocularity, and constancy Kenneth Knoblauch, (2004) 711–720. https://doi.org/10.1167/4.9.4.

[15] M. Olkkonen, D.H. Brainard, Perceived glossiness and lightness under real-world illumination, 10 (2010) 1–19. https://doi.org/10.1167/10.9.5.Introduction.

[16] M. Olkkonen, Joint effects of illumination geometry and object shape in the perception of surface reflectance, 2 (2011) 1014–1034.

[17] R.W. Fleming, R.O. Dror, E.H. Adelson, Real-world illumination and the perception of surface reflectance properties (a) (c) (b) (d), (2003) 347–368.

[18] G. Wendt, R. Mausfeld, Disparity , motion , and color information improve gloss constancy performance, 10 (2010) 1–17. https://doi.org/10.1167/10.9.7.Introduction.

[19] M.A.R. Ogers, K.E.K. Noblauch, Maximum likelihood conjoint measurement of lightness and chroma, 33 (2016) 184–193.

[20] A.C. Schmid, B.L. Anderson, Do surface reflectance properties and 3-D mesostructure influence the perception of lightness ?, 14 (2014) 1–24. https://doi.org/10.1167/14.8.24.doi.

[21] F.A.A. Kingdom, Lightness , brightness and transparency : A quarter century of new ideas , captivating demonstrations and unrelenting controversy, Vision Res. 51 (2011) 652–673. https://doi.org/10.1016/j.visres.2010.09.012.

[22] K. Doerschner, L.T. Maloney, Perceived glossiness in high dynamic range scenes, 10 (2010) 1–11. https://doi.org/10.1167/10.9.11.Introduction.

[23] S. Hansmann-Roth, P. Mamassian, A glossy simultaneous contrast: Conjoint measurements of gloss and lightness, Iperception. 8 (2017). https://doi.org/10.1177/2041669516687770.

[24] L. Qi, M.J. Chantler, J.P. Siebert, J. Dong, The joint effect of mesoscale and microscale roughness on

perceived gloss, Vision Res. 115 (2015) 209–217. https://doi.org/10.1016/j.visres.2015.04.014.

[25] I. Motoyoshi, S. Nishida, L. Sharan, E.H. Adelson, Image statistics and the perception of surface qualities, 447 (2007) 206–209. https://doi.org/10.1038/nature05724.

[26] A.C. Chadwick, R.W. Kentridge, The perception of gloss : A review, Vision Res. 109 (2015) 221–235. https://doi.org/10.1016/j.visres.2014.10.026.

[27] C. Measurement, O.F. Gloss, Conjoint measurement of gloss and surface, 19 (2009) 196–204. https://doi.org/10.1111/j.1467-9280.2008.02067.x.CONJOINT.

[28] S. Ignell, U. Kleist, M. Rigdahl, On the relations between color, gloss, and surface texture in injection-molded plastics, Color Res. Appl. 34 (2009) 291–298. https://doi.org/10.1002/col.20510.

[29] S. Ignell, U. Kleist, M. Rigdahl, Visual perception and measurements of texture and gloss of injection-molded plastics, Polym. Eng. Sci. 49 (2009) 344–353. https://doi.org/10.1002/pen.21279.

[30] I. Ariño, U. Kleist, M. Rigdahl, Effect of gloss and texture on the color of injection-molded pigmented plastics, Polym. Eng. Sci. 45 (2005) 733–744. https://doi.org/10.1002/pen.20330.

[31] J. Macher, D.P. Gruber, T. Altenbuchner, G.A. Pacher, G.R. Berger, W. Friesenbichler, A novel sink mark model for high gloss injection molded parts - Correlation of deflectometric and topographic measurements, Polym. Test. 39 (2014) 12–19. https://doi.org/10.1016/j.polymertesting.2014.07.001.

[32] T.B. Nguyen Thi, A. Yokoyama, S. Hamanaka, K. Kodama, K. Yamashita, C. Nonomura, Numerical and experimental evaluation of surface properties of embossed decorative injection-molded parts, Polym. Test. 53 (2016) 188–196. https://doi.org/10.1016/j.polymertesting.2016.05.021.

[33] C.A. Griffiths, A. Rees, R.M. Kerton, O. V. Fonseca, Temperature effects on DLC coated micro moulds, Surf. Coatings Technol. 307 (2016) 28–37. https://doi.org/10.1016/j.surfcoat.2016.08.034.

[34] J. Dufils, F. Faverjon, C. Héau, C. Donnet, Combination of laser surface texturing and DLC coating on PEEK for enhanced tribological properties, Surf. Coatings Technol. 329 (2017) 29-41. http://dx.doi.org/10.1016/j.surfcoat.2017.09.028

[35] P. Gamonal-Repiso, M. Sánchez-Soto, S. Santos-Pinto, M.L. Maspoch, Improvement of the replication quality of randomly micro-textured injection-moulding components using a multi-scale surface analysis, J. Manuf. Process. 42 (2019) 67–81. https://doi.org/10.1016/j.jmapro.2019.04.010.

[36] C.A. Brown, H.N. Hansen, X.J. Jiang, F. Blateyron, J. Berglund, N. Senin, T. Bartkowiak, B. Dixon, G. Le Goïc, Y. Quinsat, W.J. Stemp, M.K. Thompson, P.S. Ungar, E.H. Zahouani, Multiscale analyses and characterizations of surface topographies, CIRP Ann. 67 (2018) 839–862. https://doi.org/10.1016/j.cirp.2018.06.001.

[37] ISO 25178-2, Geometrical Product Specifications (GPS) - Surface texture: Areal - Part 2: Terms, definitions and surface texture parameters, First ed., 2012. [38] F. Blateyron, New 3D parameters and filtration techniques for surface metrology, Qual. Mag. (2006) 1–7.

[39] R.J. Woodham, Photometric Method For Determining Surface Orientation From Multiple Images, Opt. Eng. 19 (1980) 139–144. https://doi.org/10.1117/12.7972479.

[40] E. F. Taylor. Illumination fundamentals. Rensselaer, 2000.

[41] F.W. Campbell, R.W. Gubisch, Optical quality of the human eye, The journal of physiology. 186 (1966) 558–578 .

[42] G. Tosello, H. Haitjema, R.K. Leach, D. Quagliotti, S. Gasparin, H.N. Hansen, An international comparison of surface texture parameters quantification on polymer artefacts using optical instruments, CIRP Ann. - Manuf. Technol. 65 (2016) 529–532. https://doi.org/10.1016/j.cirp.2016.04.003.

[43] JCGM 100:2008, Evaluation of measurement data – Guide to the expression of uncertainty in measurement, Jt. Comm. Guid. Metrol. (2008). https://doi.org/10.1373/clinchem.2003.030528.

[44] F. Nicodemus, J. Richmond, J. Hsia, Geometrical considerations and nomenclature for reflectance, Sci. Technol. 60 (1977) 1–52. https://doi.org/10.1109/LPT.2009.2020494.

[45] P. Gamonal-Repiso, M. Sánchez-Soto, S. Santos-Pinto, M.L. Maspoch, Influence of topography on the scratch and mar visibility resistance of randomly micro-textured surfaces, Wear. 440–441 (2019). https://doi.org/10.1016/j.wear.2019.203082.

[46] F. Leloup, P. Hanselaer, J. Versluys, S. Forment, BRDF and gloss measurements, CIE Expert Symp. (2007) 1–6.

Table Captions

Table 1: Uncertainty contribution to the TAM prototype instrument.

Table 2: Topographic results of each texture finish measured with the CWL sensor and took as reference for TAM setting.

Table 3: Settings and topographical results obtained with TAM prototype.

Table 4: Isotropy results of the four textures under study at the macro-scale.

Table 5: Topographic results at the limited scale S-L 0.04 – 5.

Table 6: Results of gloss measurements at 60º.

Table 7: Results of the texture slope (TS) and texture aperture angle (TAA) of the four texture finishes.

Figure Captions

Figure 1. Surface micrograph of the four surfaces under study. (a) texture A, (b) texture B, (c) texture C and (d) texture D.

Figure 2. Scheme of the distribution of the different functional parameters, reduced peak height (Spk), core roughness (Sk) and reduced dale height (Svk).

Figure 3. Methodology to determine the isotropy of the surface. (a) Reconstruction of the original surface in 3D; (b) resultant surface after applying the autocorrelation function (ACF); (c) maximum and minimum radii measurement of the lobe.

Figure 4. Surface reflectivity performance as a function of the functional height parameters.

Figure 5. Texture slope (TS) and texture aperture angle (TAA) measurement methodology. The TS is the slope of the cell wall and the TAA is the angle created by two neighbour cells. Both are extracted from the 3D reconstruction (a).

Figure 6. Measuring principle of the photometric stereo (PS) technology and reconstruction of the surface in three dimensions (3D).

Figure 7. Measurement locations.

Figure 8. Effect of the filter offset on the cells segmentation. (a) Under segmentation, filter offset = 5, detecting 47 cells. (b) Over segmentation, filter offset = 50, detecting 302 cells.

Figure 9. Results of roughness at different limited scales. (a) arithmetic roughness and (b) root mean square roughness.

Figure 10. SEM images of (a) texture A, (b) texture B, (c) texture C and (d) texture D.

Figure 11. Results of reflectivity in both peaks and valleys of the four surface finishes.

Figure 12. Reflectivity map of (a) texture A, (b) texture B, (c) texture C and (d) texture D.

Figure 1a

Click here to access/download;Figure;Figura_1a.tif

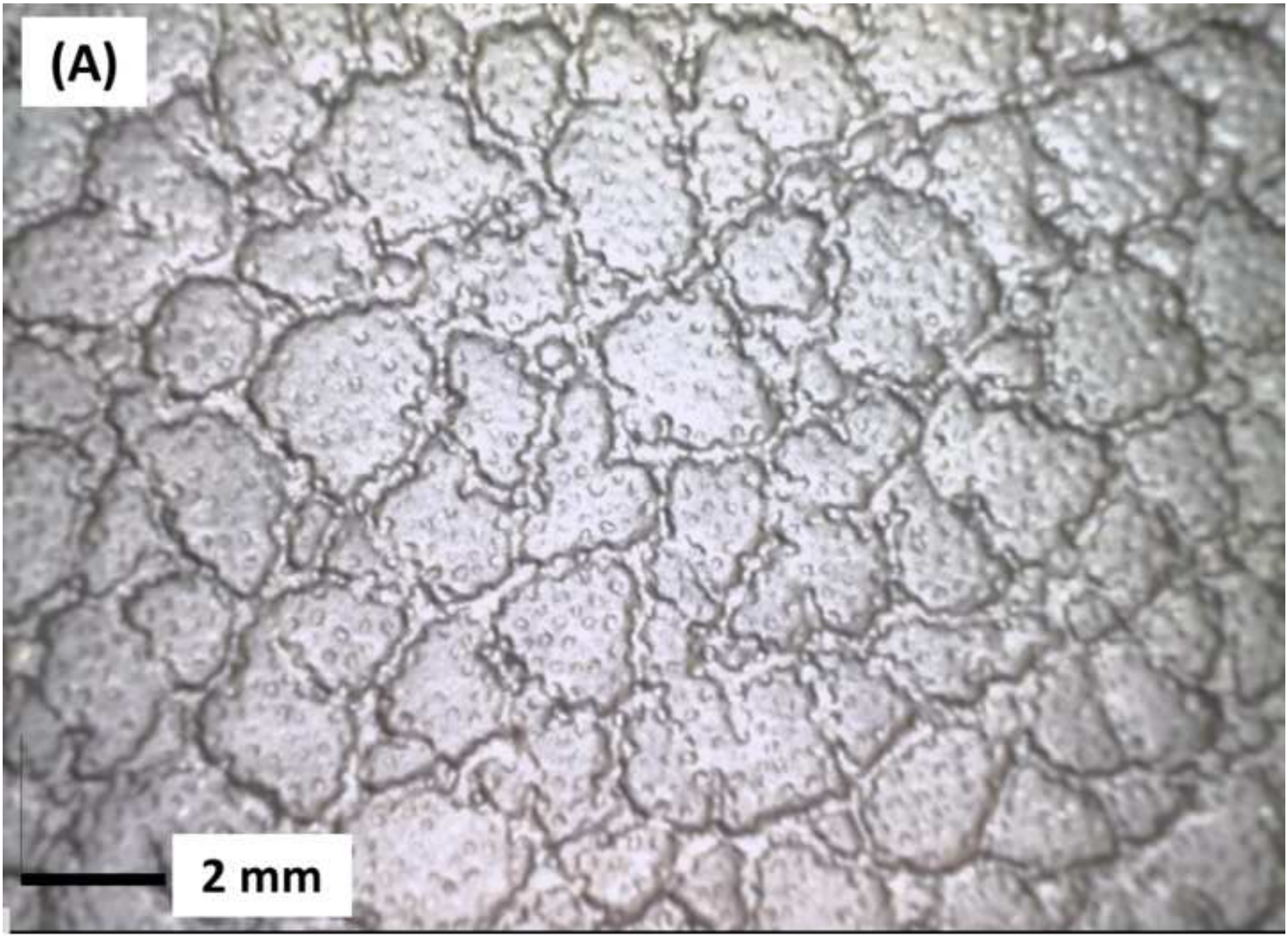

Figure 1b

Click here to access/download;Figure;Figura_1b.tif

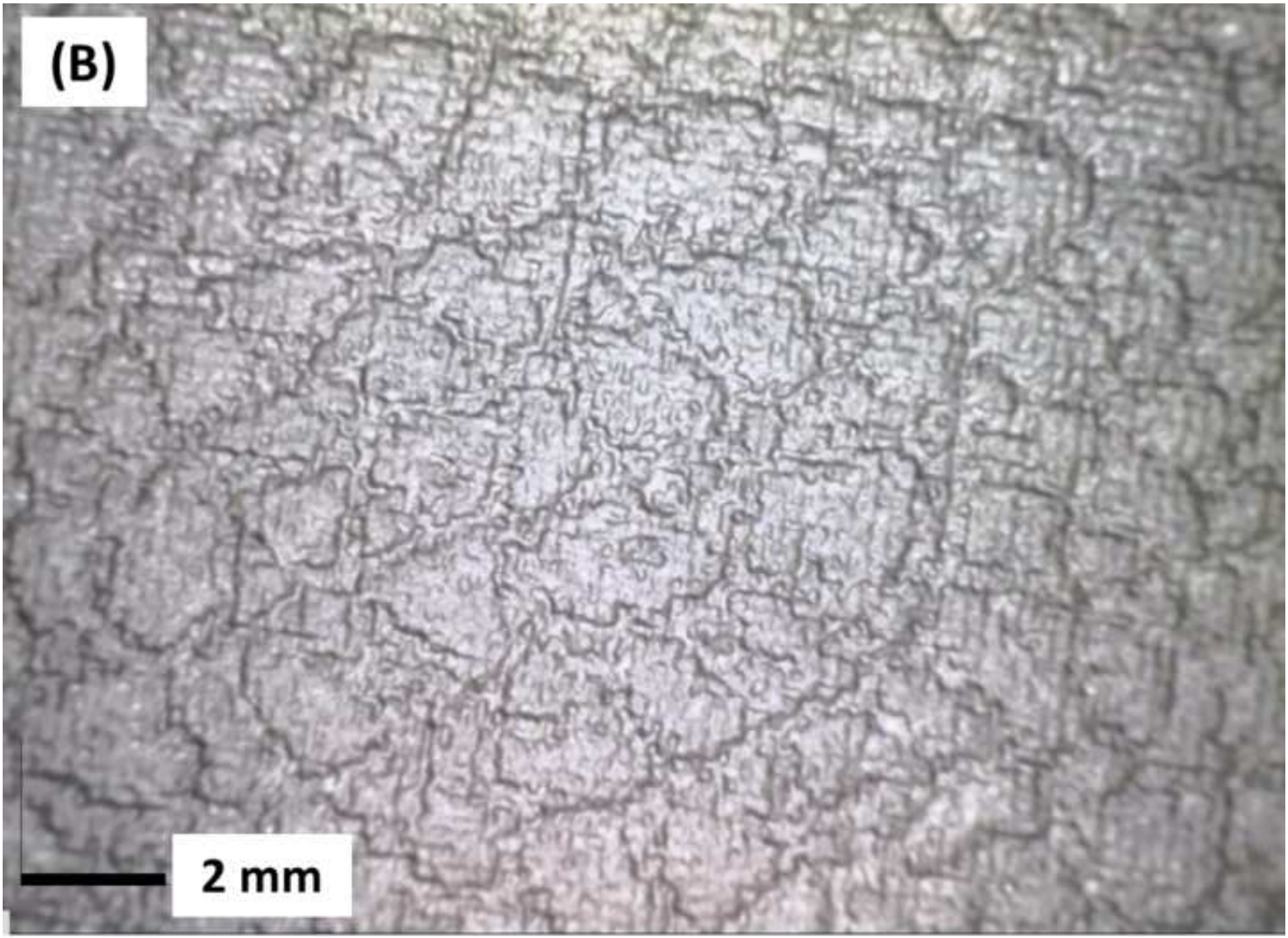

Figure 1c

Click here to access/download;Figure;Figura_1c.tif

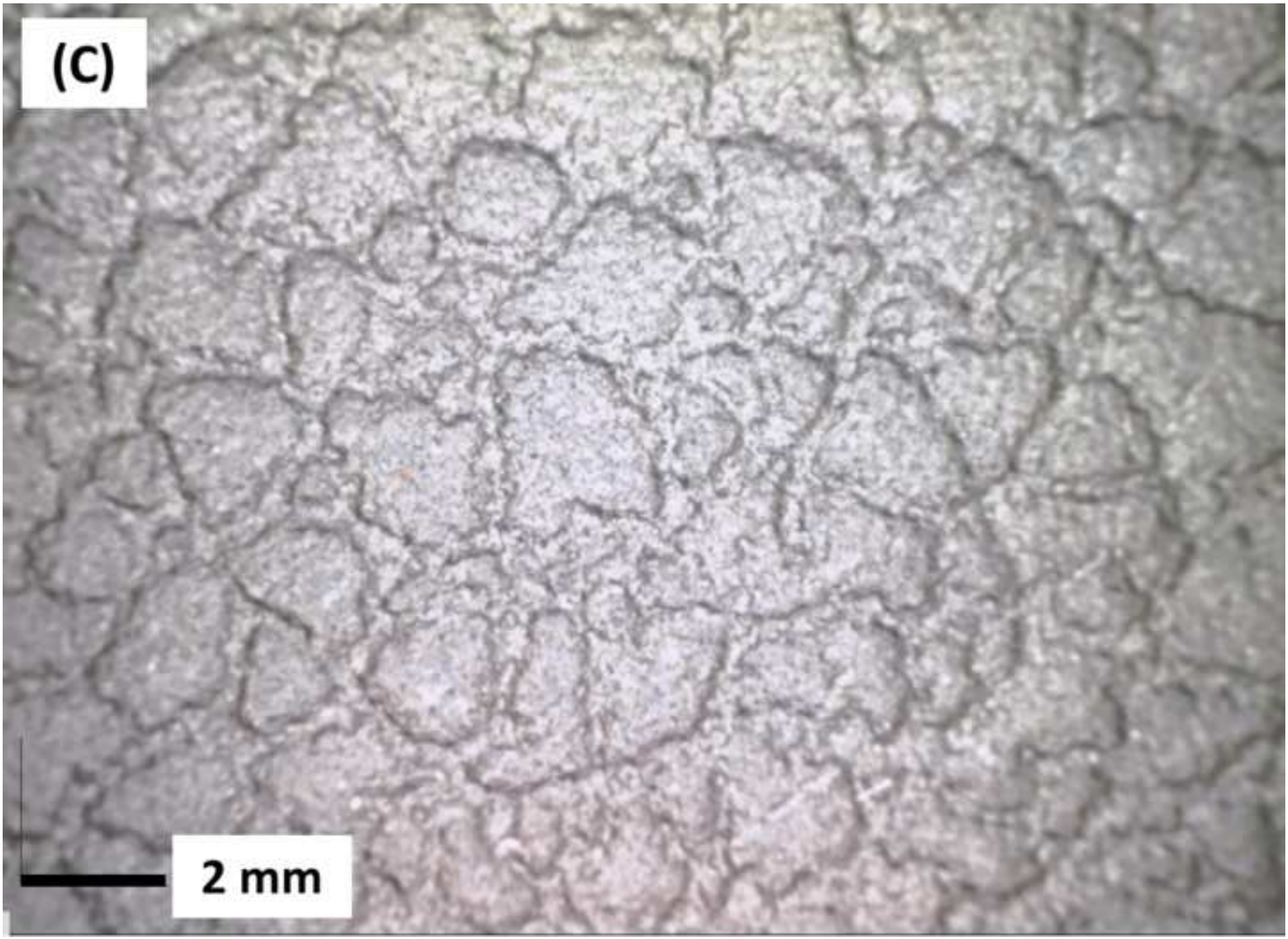

Figure 1d

Click here to access/download;Figure;Figura_1d.tif

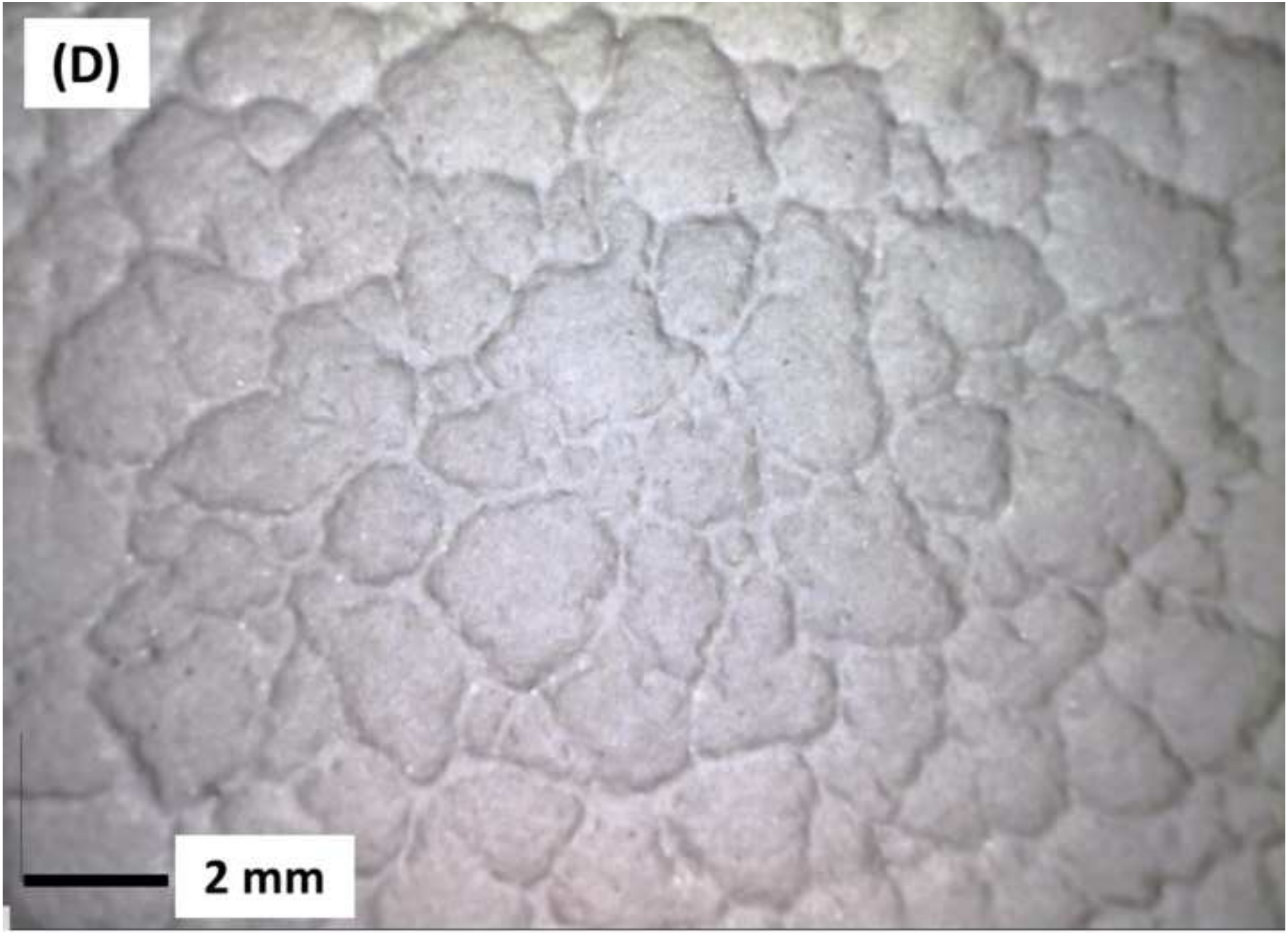

Figure 2

Click here to access/download;Figure;Figure_2.tif

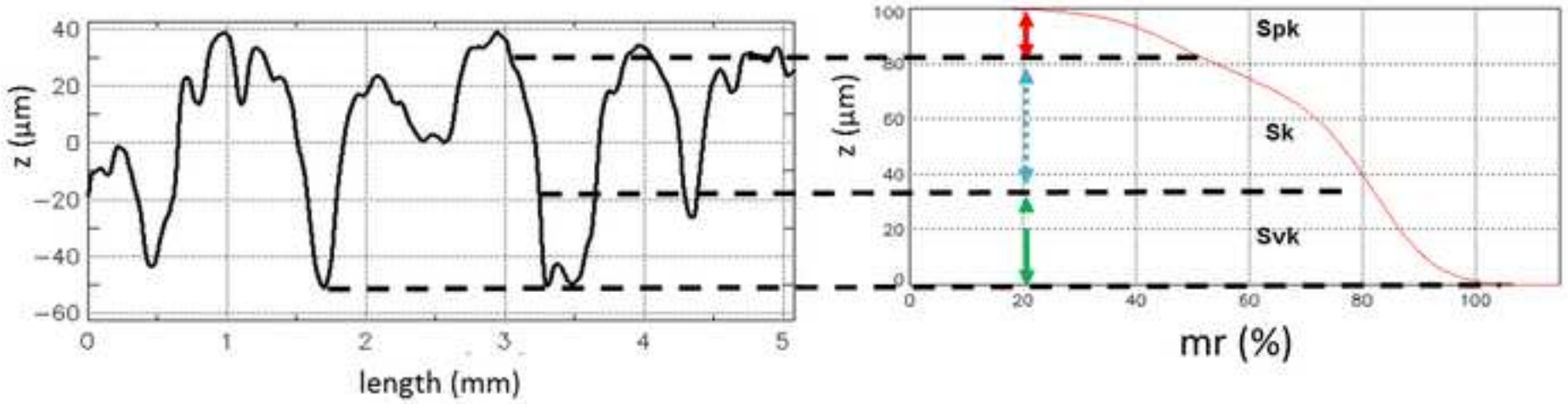

Figure_3

Click here to access/download;Figure;Figure_3.tif

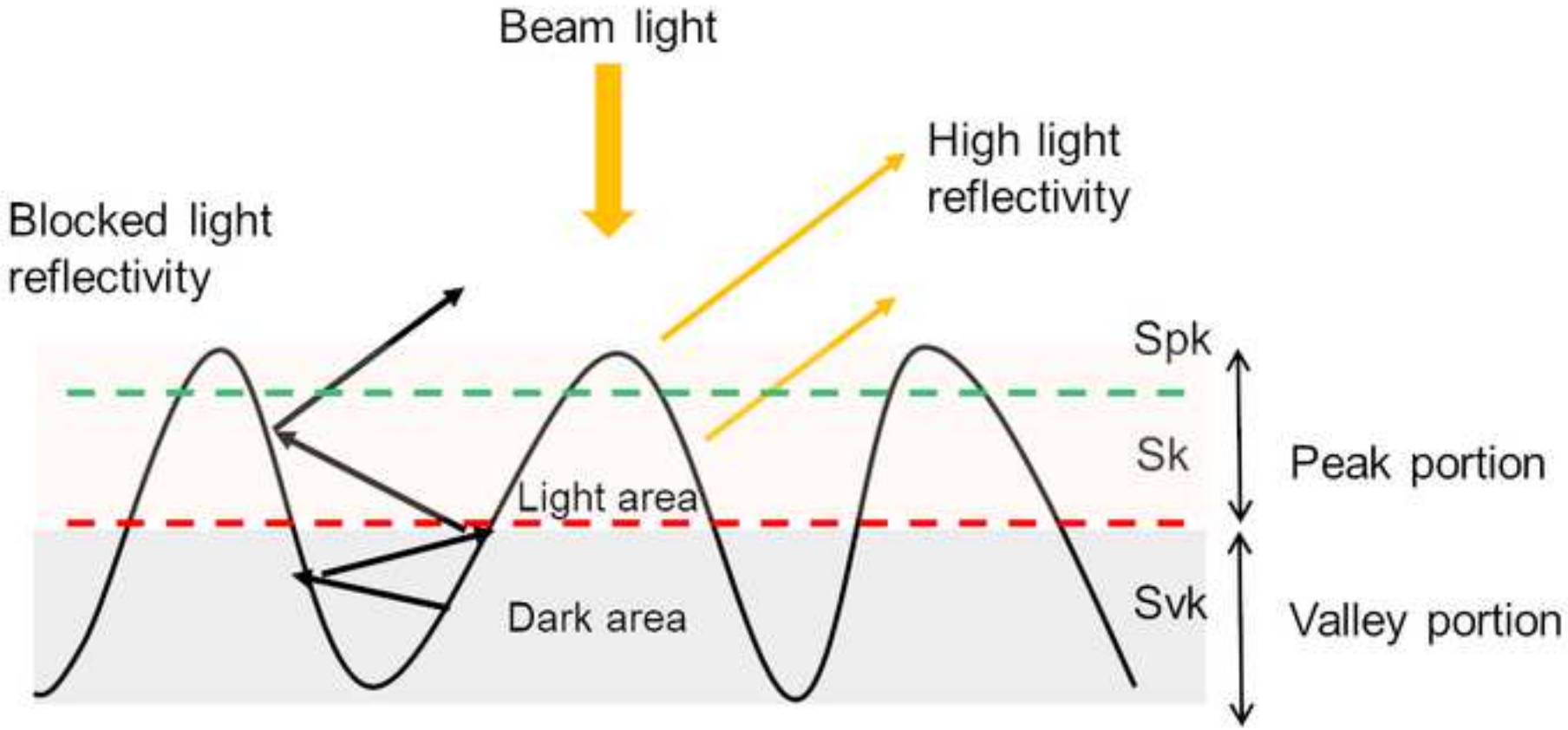

Figure_4

Click here to access/download;Figure;Figure_4.tif

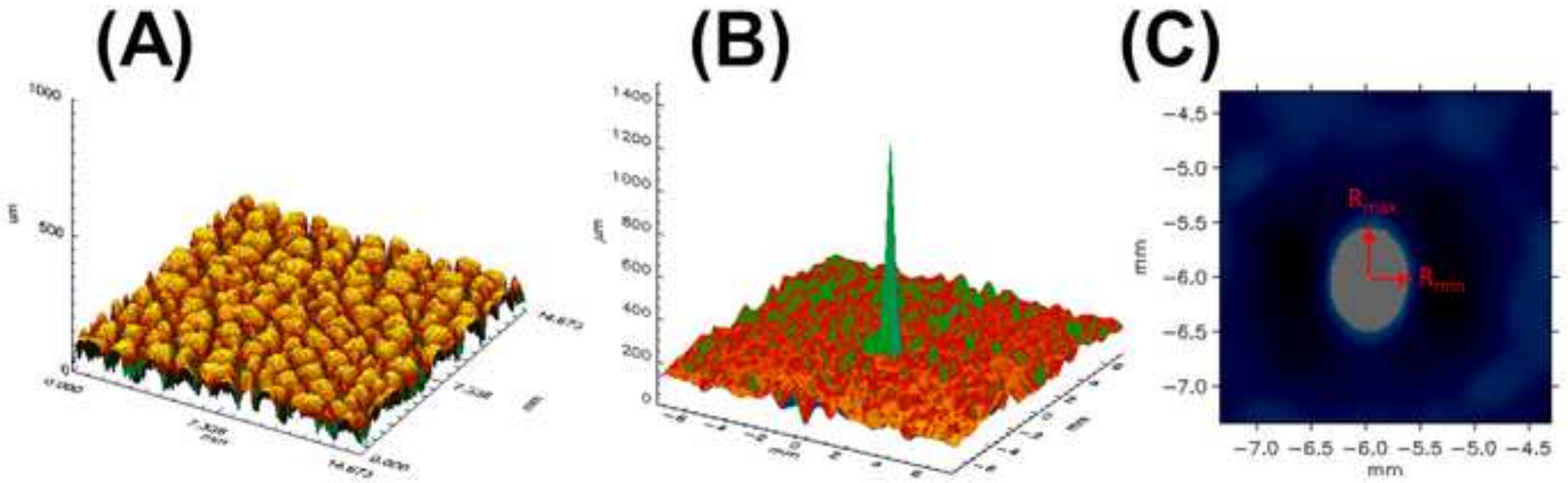

Figure_5

Click here to access/download;Figure;Figure_5.tif

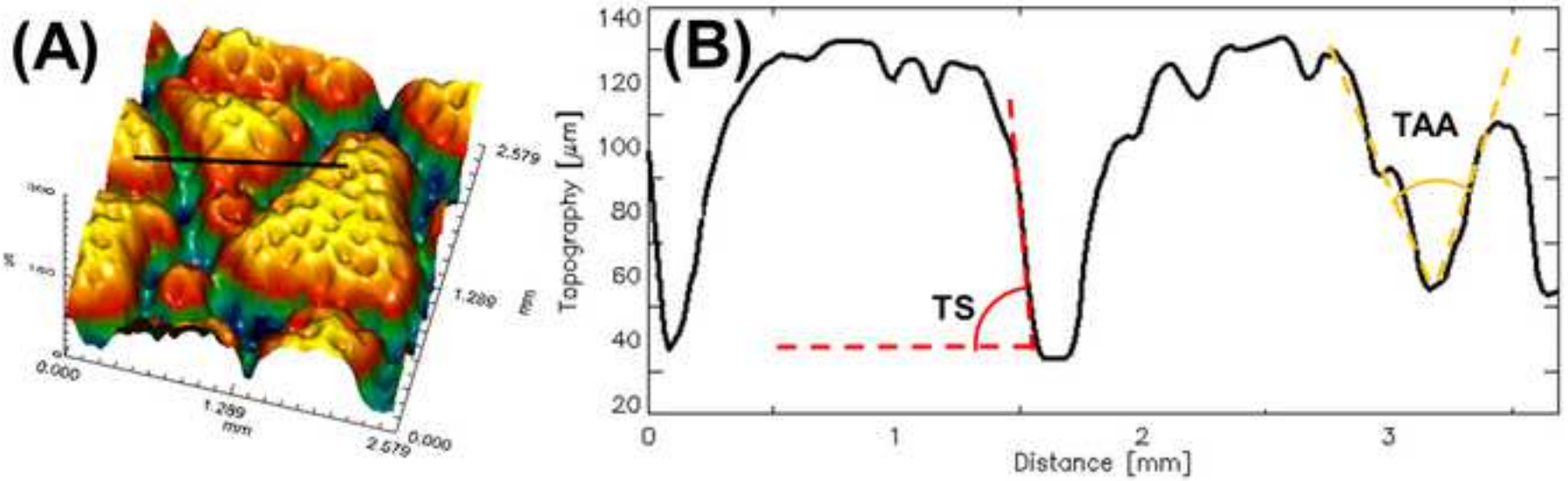

Click here to access/download;Figure;Figure_6.tif

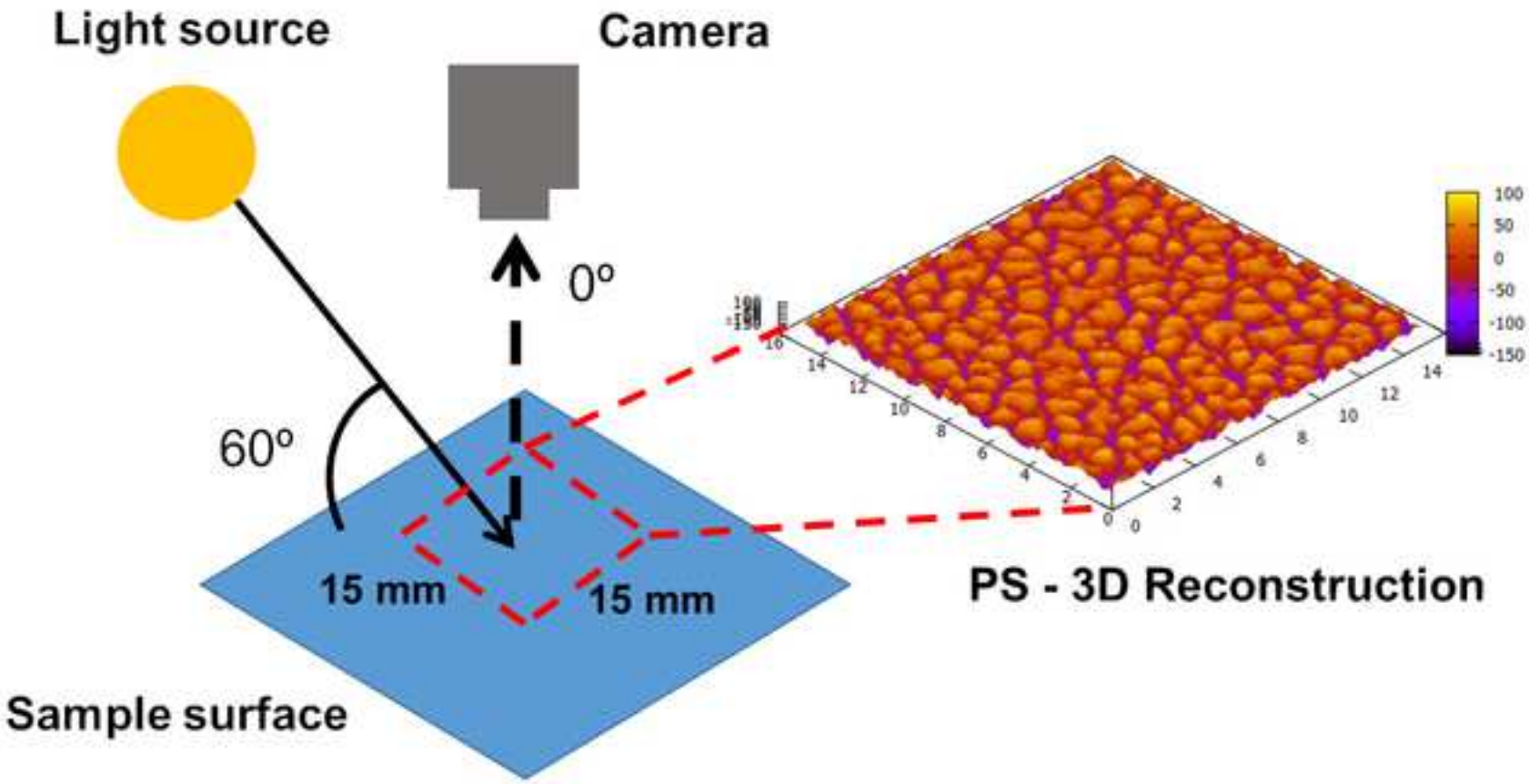

Figure_7

Click here to access/download;Figure;Figure_7_def.tif

Figure_8a

Click here to access/download;Figure;Figure_8a_def.tif

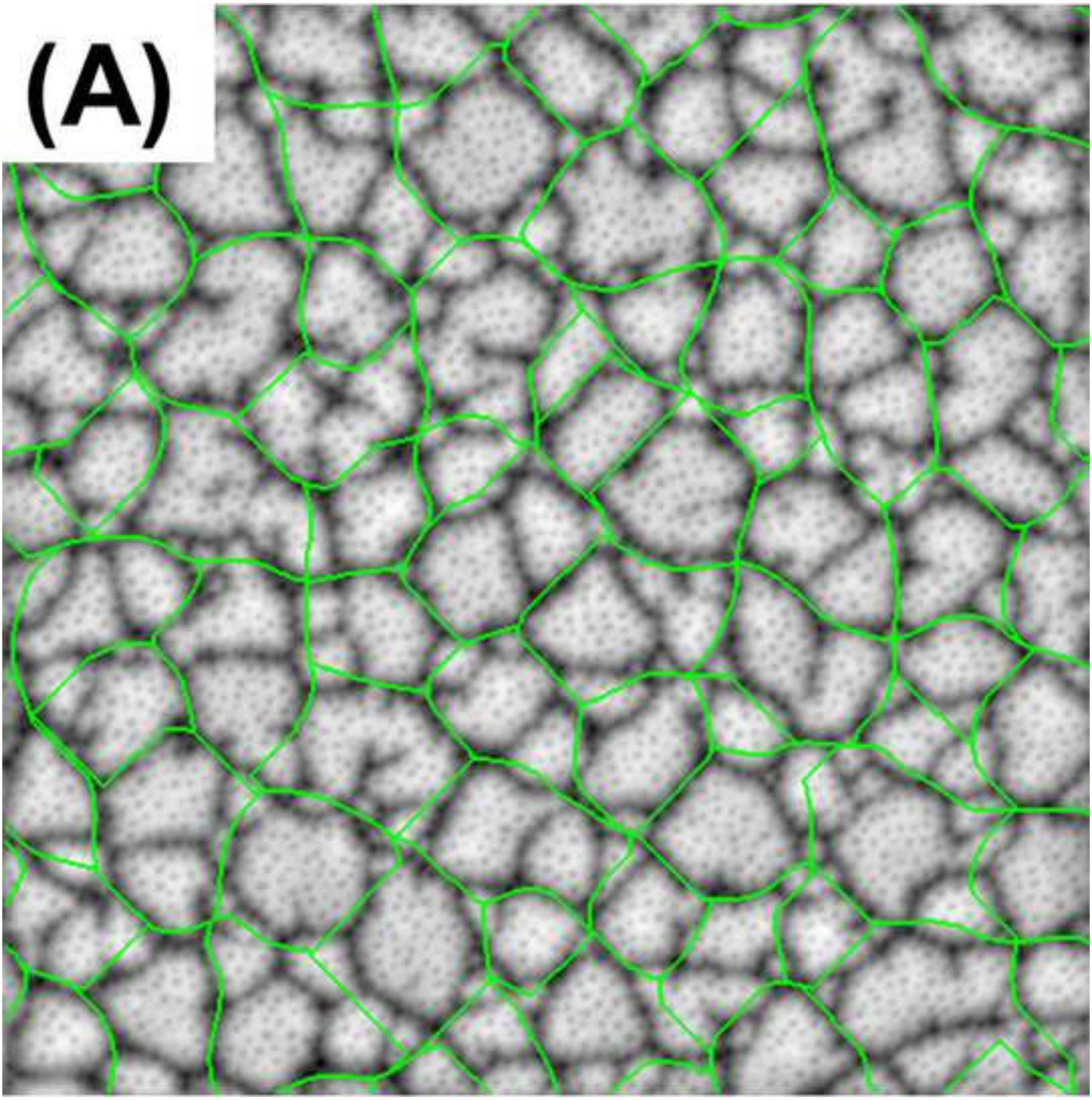

Figure_8b

Click here to access/download;Figure;Figure_8b_def.tif

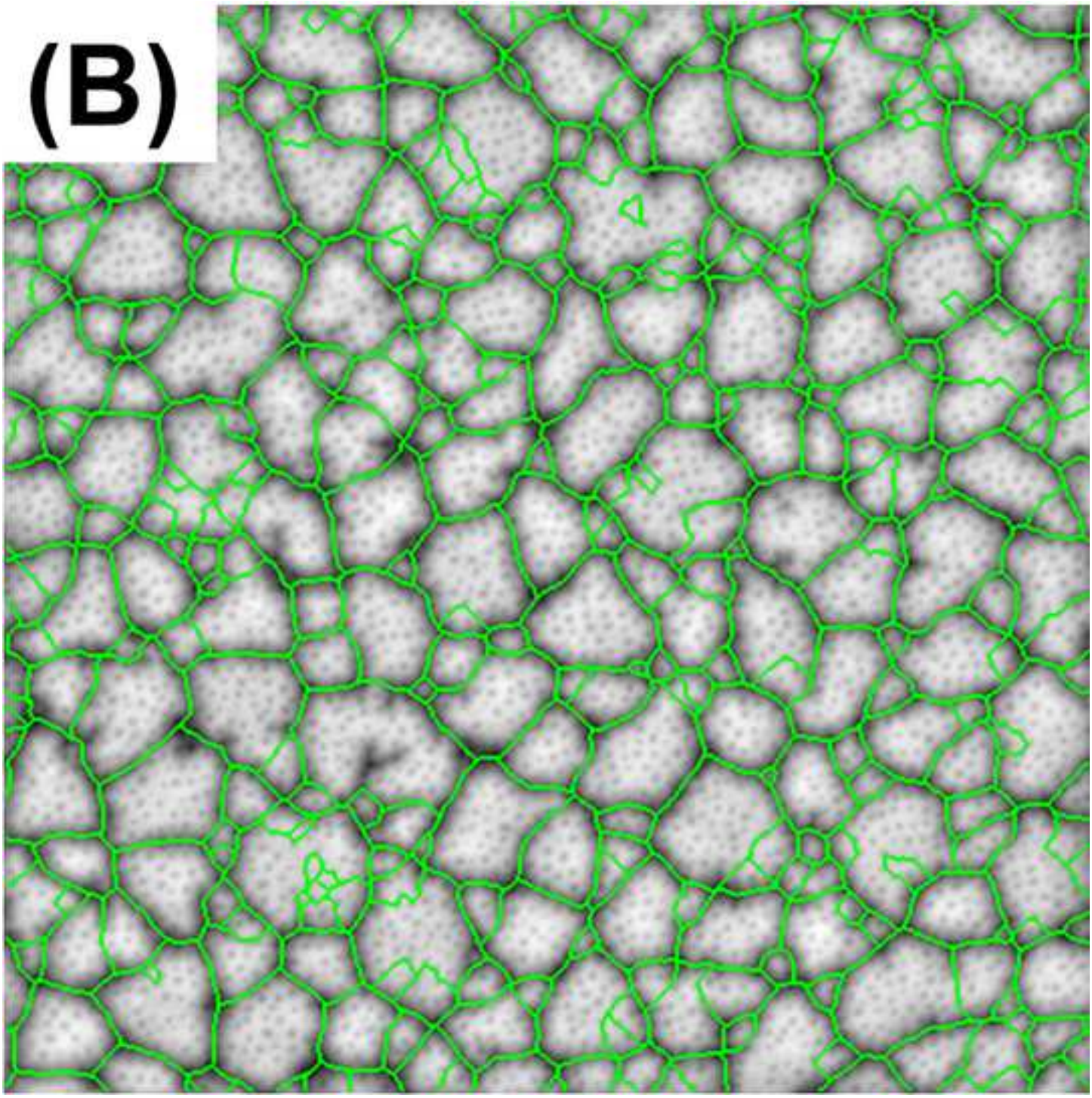

Figure_9a

Click here to access/download;Figure;Figure_9a_def.tif

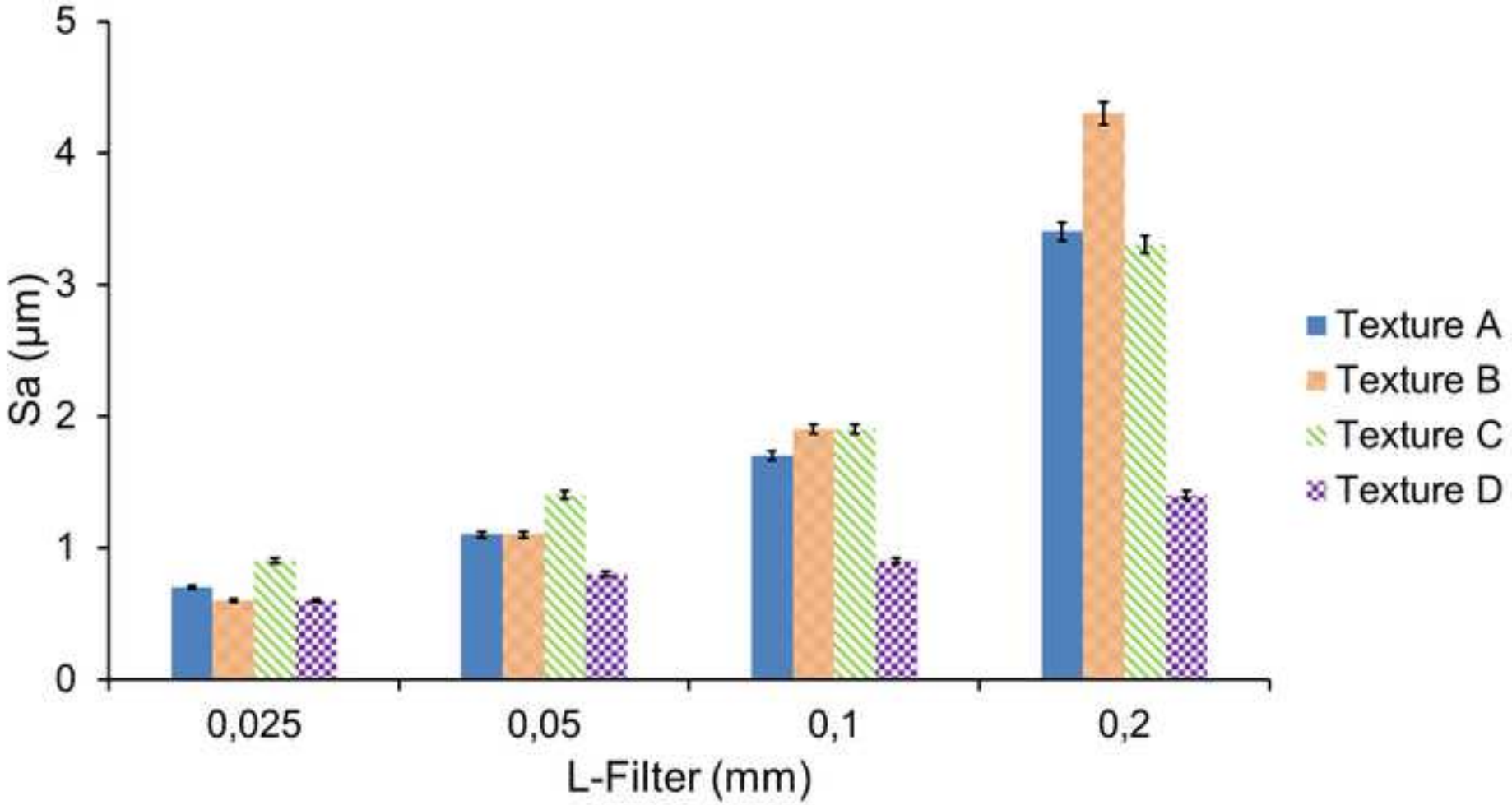

Figure_9b

Click here to access/download;Figure;Figure_9b_def.tif

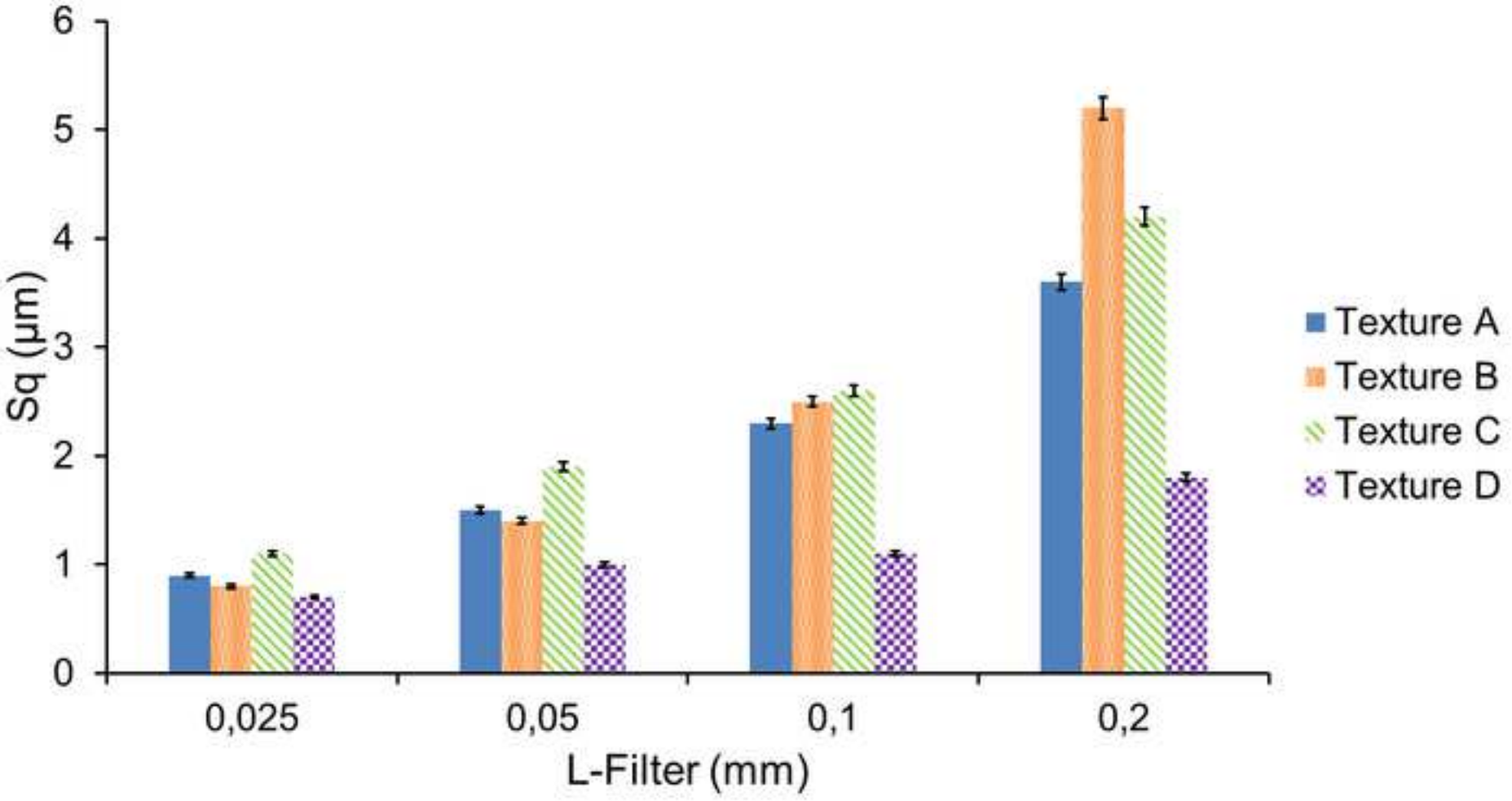

Figure_10a

Click here to access/download;Figure;Figure_10a.tif

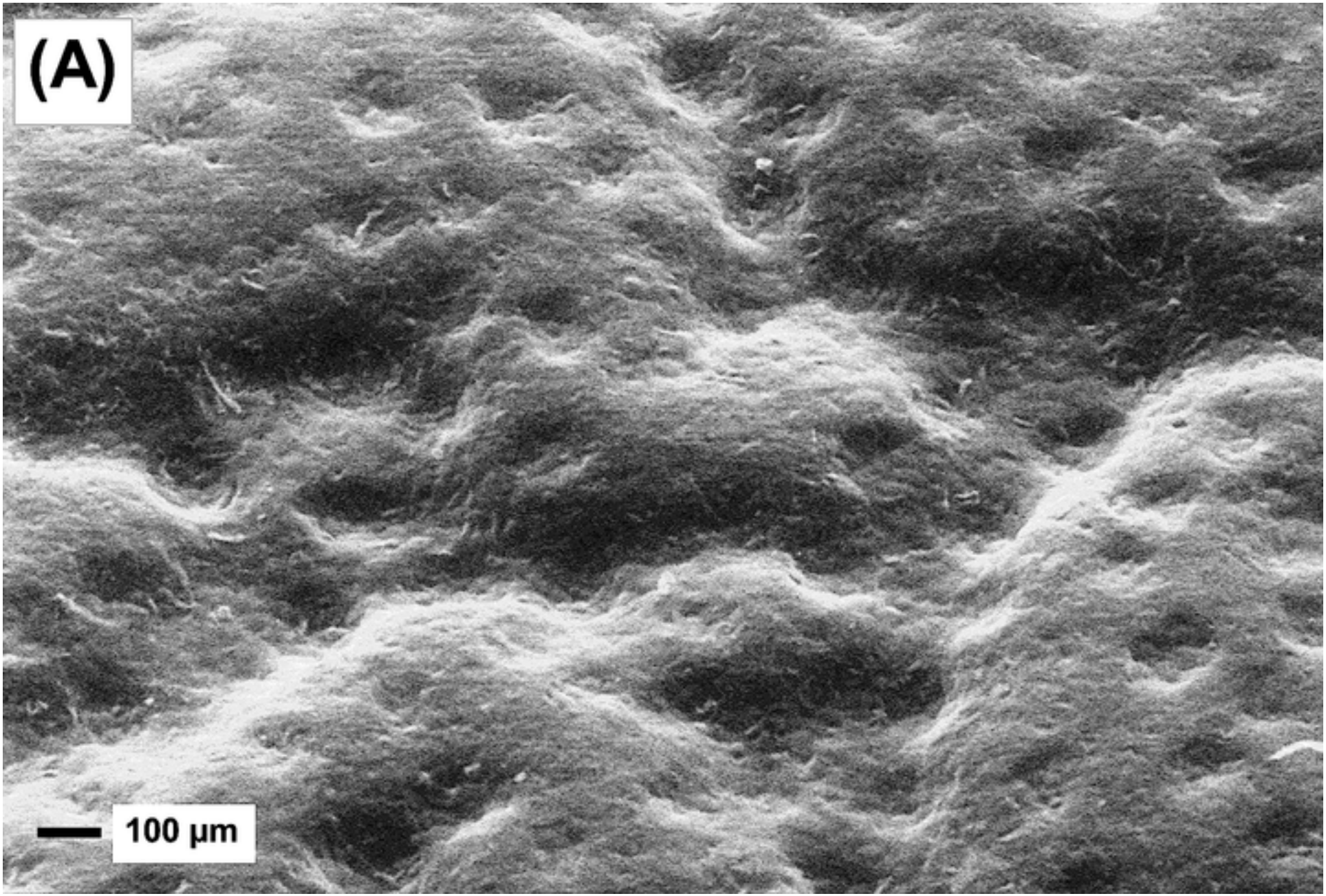

Figure_10b

Click here to access/download;Figure;Figure_10b.tif

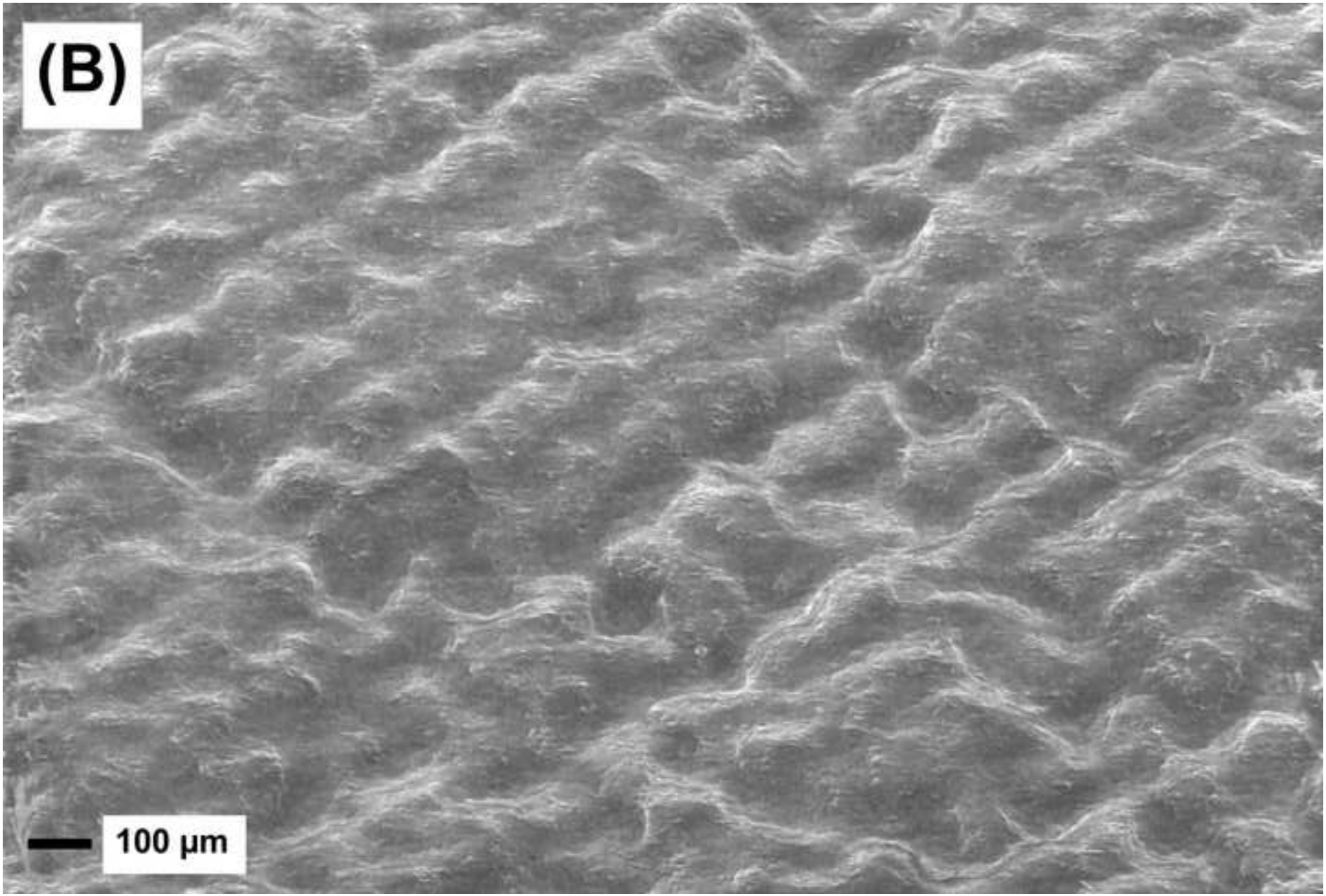

Figure_10c

Click here to access/download;Figure;Figure_10c.tif

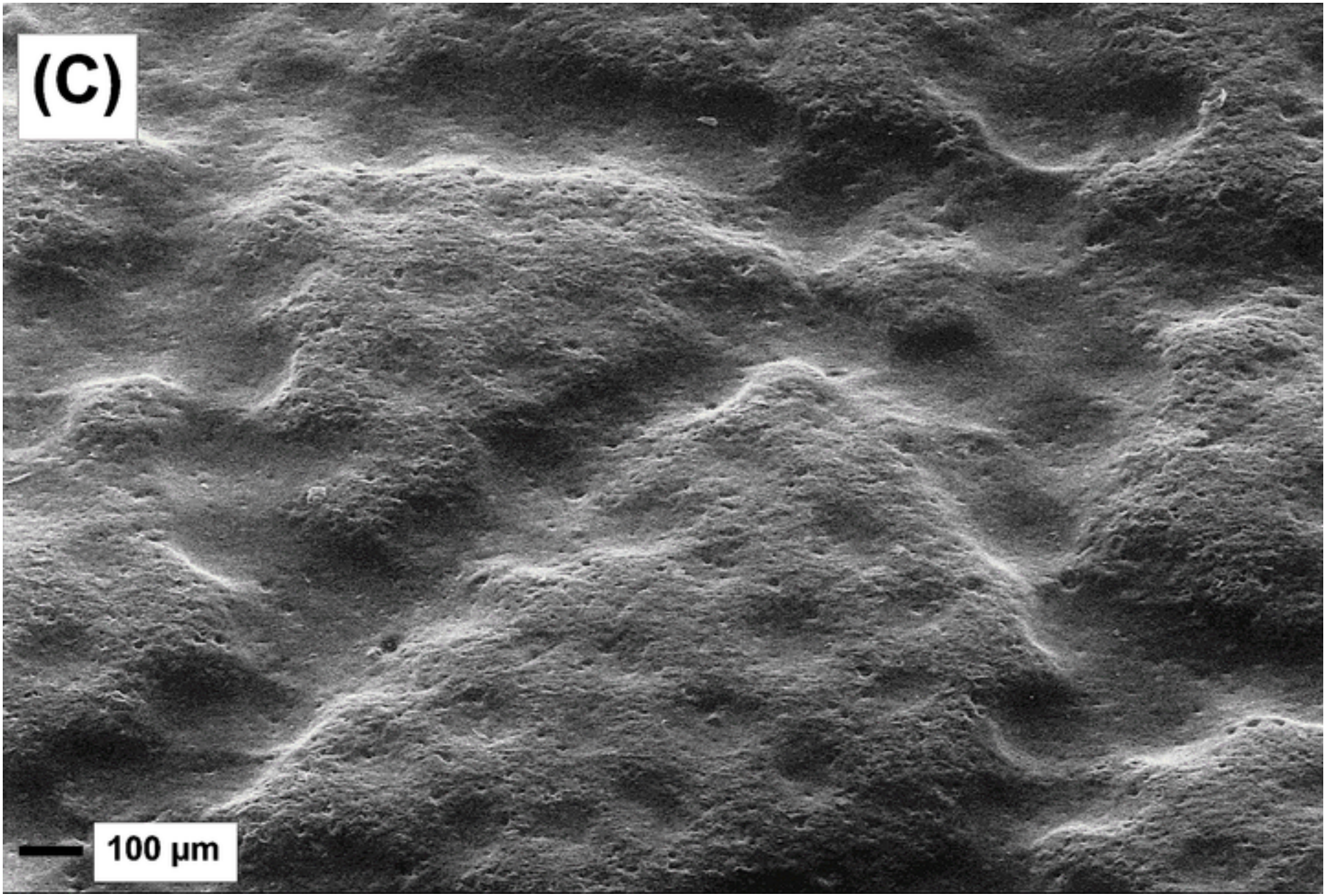

Figure_10d

Click here to access/download;Figure;Figure_10d.tif

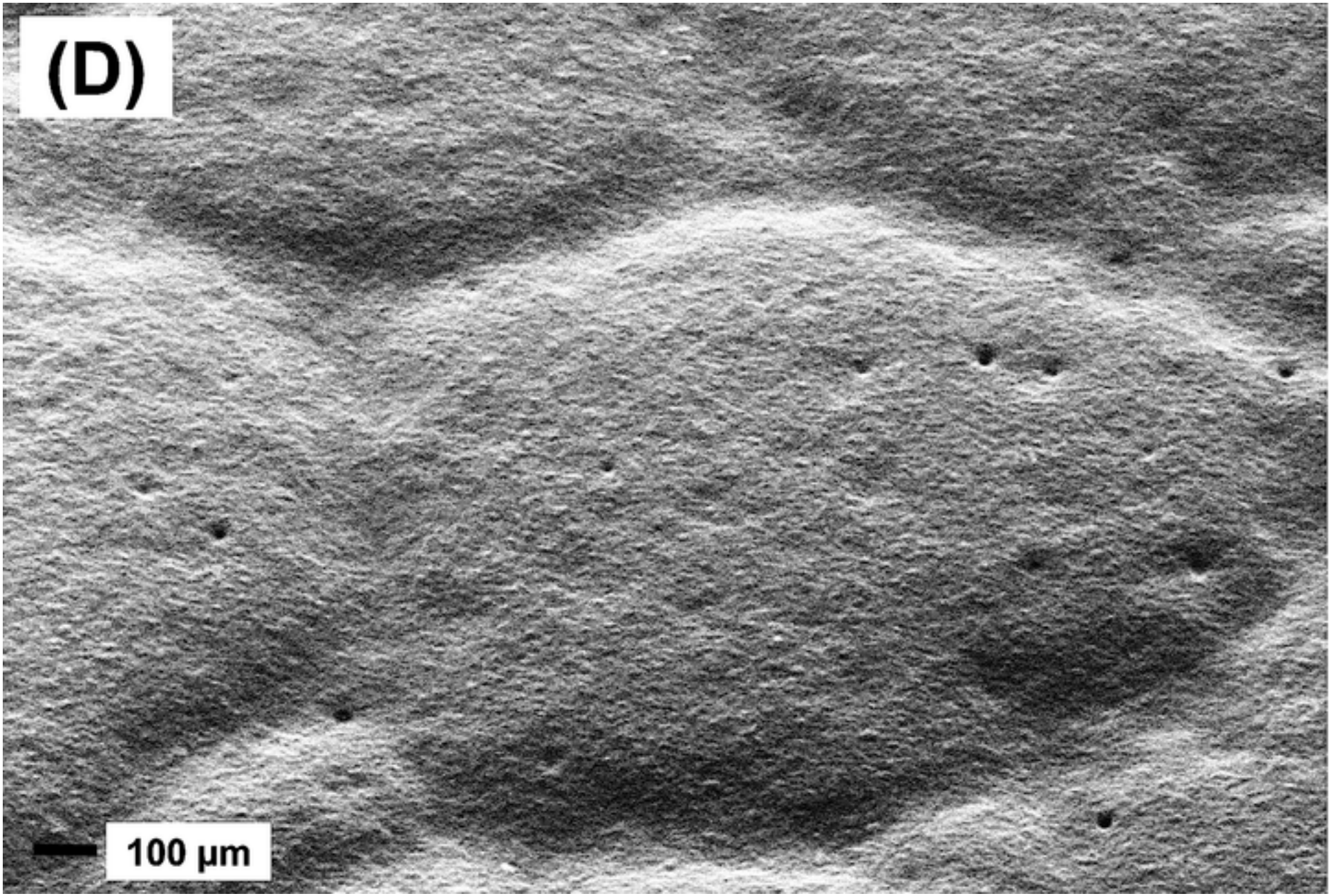

Figure_11

Click here to access/download;Figure;Figure_11.tif

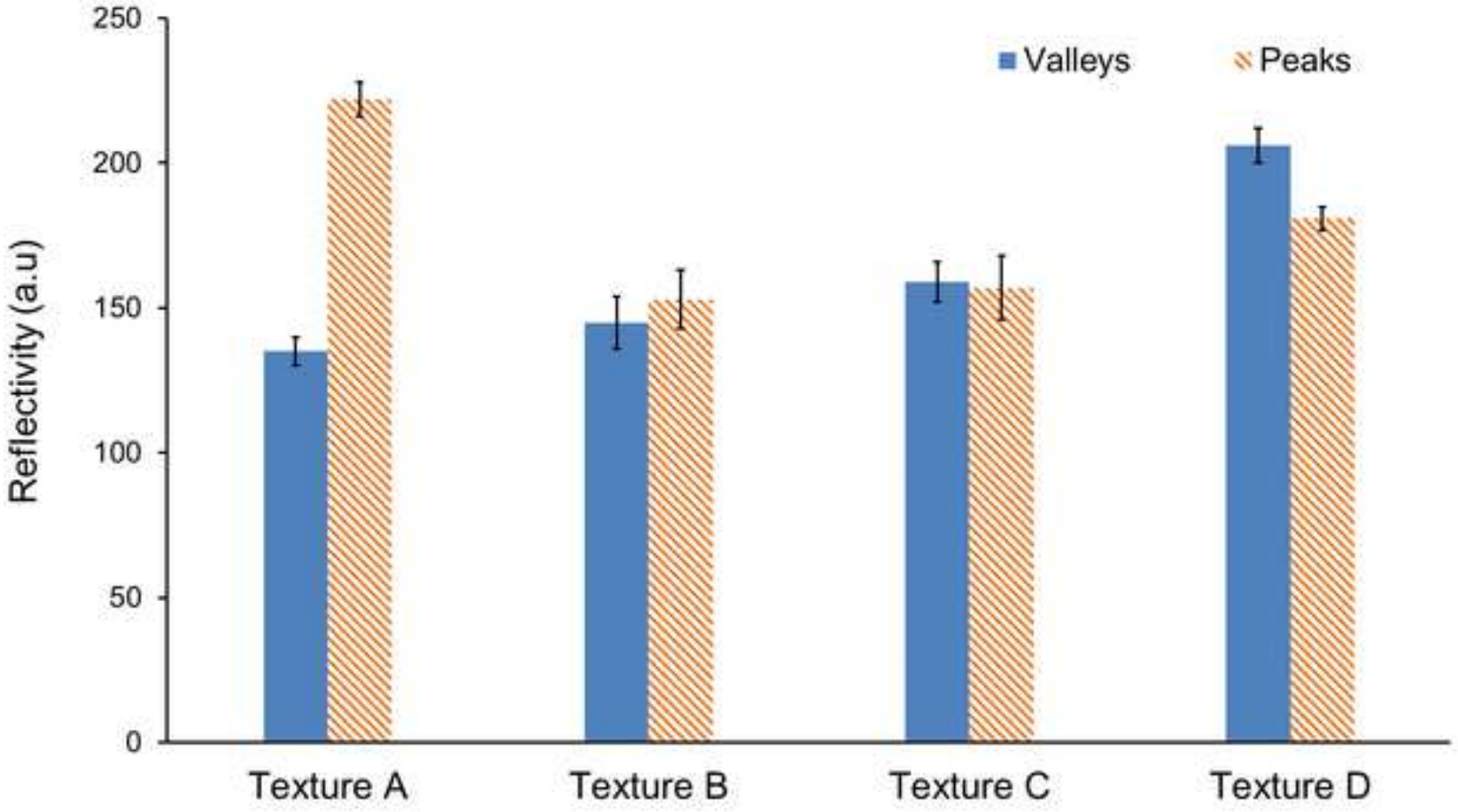

Figure_12a

Click here to access/download;Figure;Figure_12a_def.tif

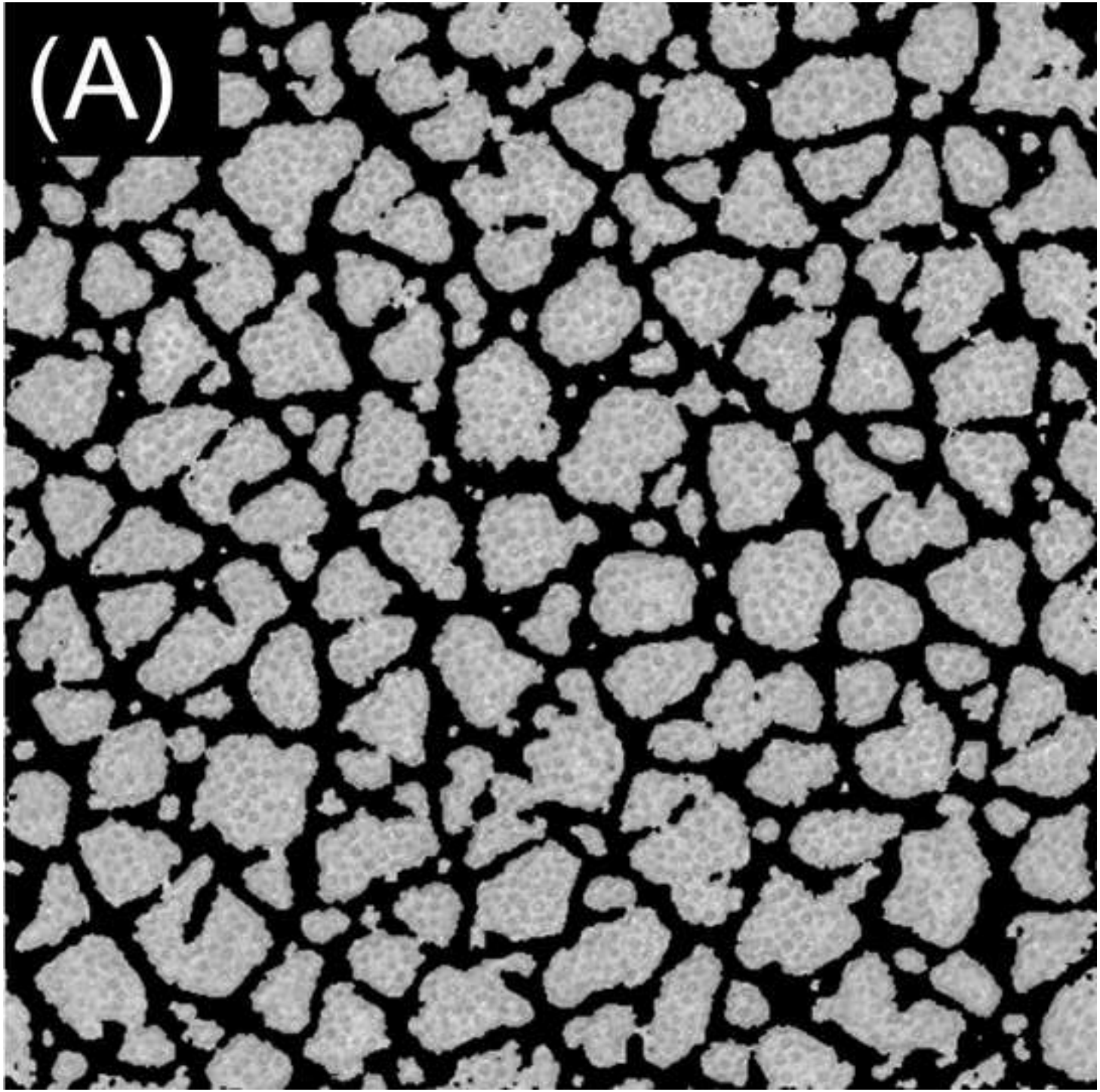

Figure_12b

Click here to access/download;Figure;Figure_12b_def.tif

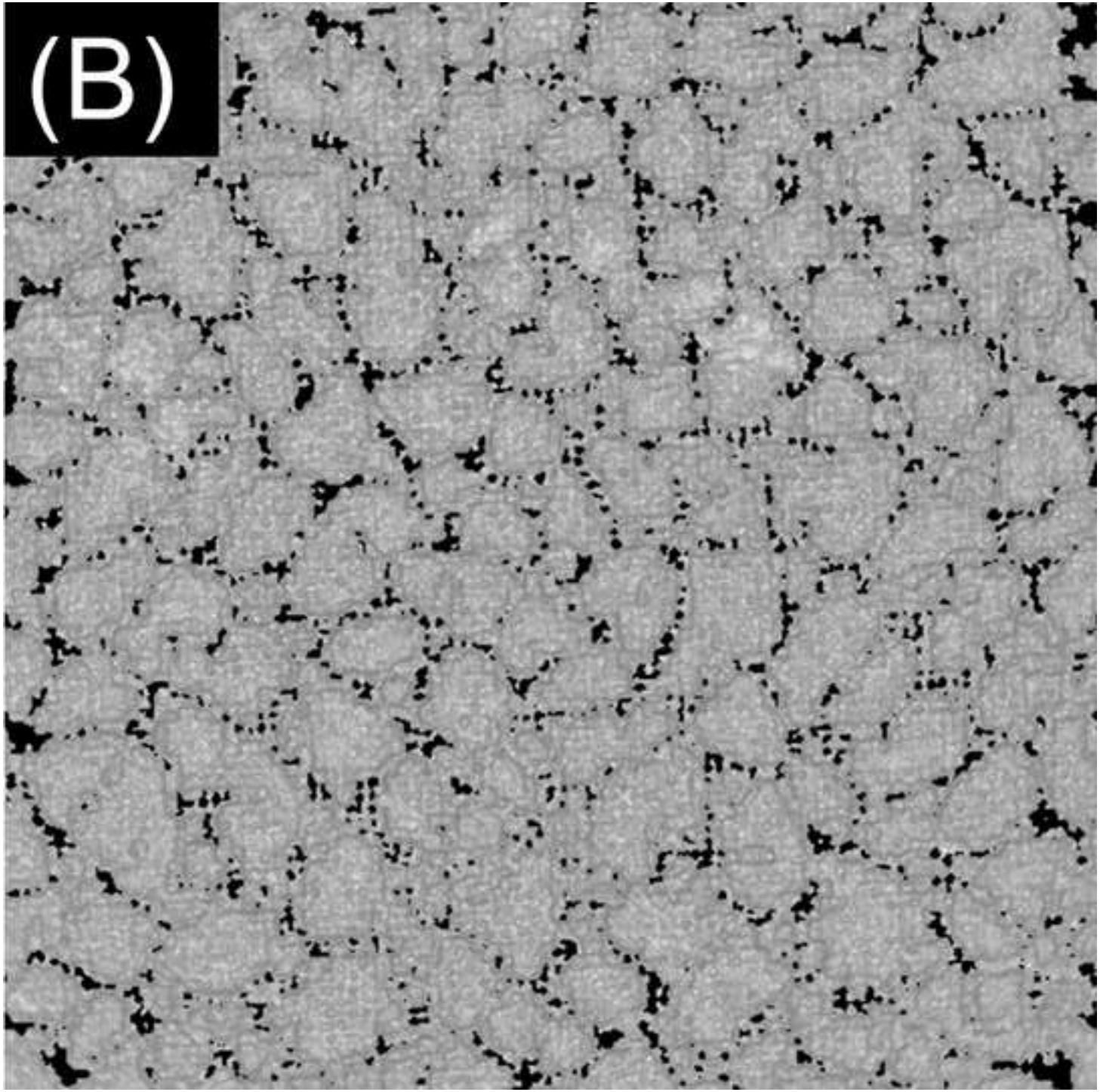

Figure_12c

Click here to access/download;Figure;Figure_12c_def.tif

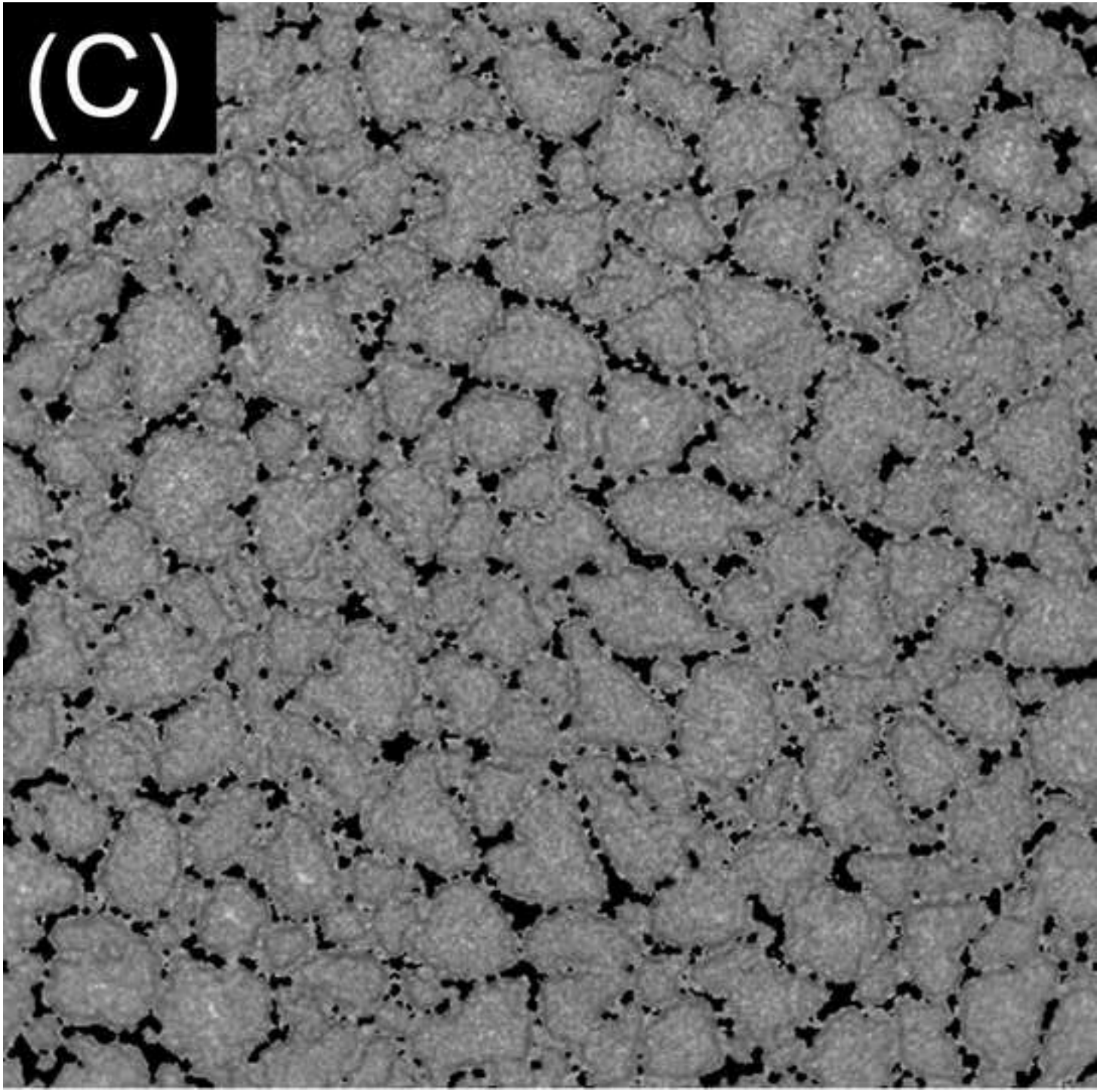

Figure_12d

Click here to access/download;Figure;Figure_12d_def.tif

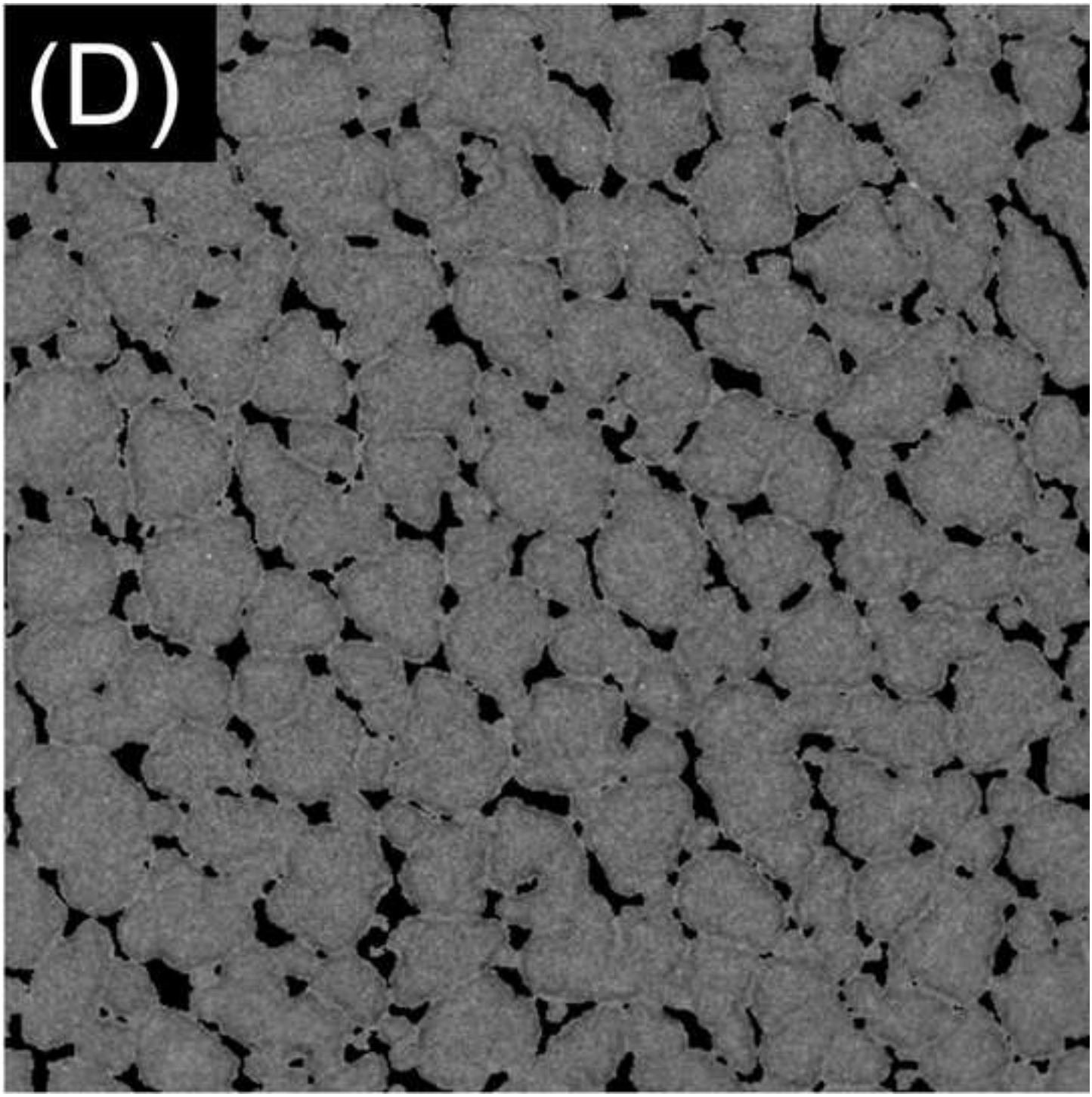

Declaration of interests

☒ The authors declare that they have no known competing financial interests or personal relationships that could have appeared to influence the work reported in this paper.

☐The authors declare the following financial interests/personal relationships which may be considered as potential competing interests:

CRediT author statement

P.Gamonal-Repiso : , Methodology, Investigation and Writing- Original draft preparation. **M. Sancez-Soto:** Conceptualization and Data curation**. T. Abt:** Visualization and Writing- Reviewing**. S. Santos-Pinto:** Supervision**. M. Ll. Maspoch:** Project administration, Supervision